Advances in Applied Energy 4 (2021) 100070

Contents lists available at ScienceDirect

Advances in Applied Energy

journal homepage: www.elsevier.com/locate/adapen

Progress in solid-state high voltage lithium-ion battery electrolytes

Anwar Ahniyaz[a,*], Iratxe de Meatza[b], Andriy Kvasha[b], Oihane Garcia-Calvo[b], Istaq Ahmed[c], Mauro Francesco Sgroi[d], Mattia Giuliano[d], Matteo Dotoli[d], Mihaela-Aneta Dumitrescu[e], Marcus Jahn[f], Ningxin Zhang[f]

[a] RISE Bioeconomy and Health Division, RISE Research Institutes of Sweden, Drottning Kristinas vag 45, P.O.Box 5607, Stockholm SE-11486, Sweden
[b] CIDETEC, Basque Research and Technology Alliance (BRTA), Paseo Miramón 196, Donostia-San Sebastián 20014, Spain
[c] Volvo Group Trucks Technology, Götaverksgatan 10, Gothenburg SE-405 08, Sweden
[d] Group Materials Labs, Environment & Chemical Analysis, C.R.F. S.C.p.A, Strada Torino 50, Orbassano (TO) 10043, Italy
[e] Faam Research Center, Lthops srl, Strada del Portone 61, Torino 10137, Italy
[f] AIT Austrian Institute of Technology GmbH, Giefinggasse 2, Vienna 1210, Austria

ARTICLE INFO

Keywords:
Solid-state battery
Electrolyte
High voltage
Lithium-ion battery
Lithium metal battery
Ionic conductor

ABSTRACT

Developing high specific energy Lithium-ion (Li-ion) batteries is of vital importance to boost the production of efficient electric vehicles able to meet the customers' expectation related to the electric range of the vehicle. One possible pathway to high specific energy is to increase the operating voltage of the Li-ion cell. Cathode materials enabling operation above 4.2 V are available. The stability of the positive electrode-electrolyte interface is still the main bottleneck to develop high voltage cells.

Moreover, important research efforts are devoted to the substitution of graphite anodes with Li metal: this would improve the energy density of the cell dramatically. The use of metallic lithium is prevented by the dendrite growth during charge, with consequent safety problems. To suppress the formation of dendrites solid-state electrolytes are considered the most promising approach.

For these reasons the present review summarizes the most recent research efforts in the field of high voltage solid-state electrolytes for high energy density Li-ion cells.

1. Introduction

Recently, there is an increasing interest in energy storage technology and batteries have been widely used as energy sources in consumer electronics, power tools and automotive sectors, resulting in intensive research and development into them [1,2]. Particularly, development of high specific energy cells and solid-state lithium secondary cells becomes the focus of these efforts [3–5].

The main purpose of the present work is to provide an overview about high voltage solid-state electrolytes, starting from the state of art of liquid electrolytes (along with the related deep knowhow in separator materials), passing through the liquid-like gel materials and arriving at the most promising solid-based electrolyte materials. We discuss and analyze advantages and drawbacks of each class of materials.

As shown in the Fig. 1, we identified five main classes of electrolytes.

1 Liquid Electrolytes (state of art of commercial Li-ion cells).
2 Gel Polymer Electrolytes.
3 Solid Polymer Electrolytes.
4 Solid Inorganic Electrolytes.
5 Hybrid Electrolytes (combination of previous ones).

Fig. 1 correlates the ionic conductivity (σ) at 25 °C with the operating voltage window of the different materials. To be suitable as an effective Li-ion cell electrolyte, an electrolyte material has to guarantee a high ionic conductivity (at least 10–3 S/cm) at cell operating temperature and a wide voltage stability window enabling operation up to 5 V vs. Li/Li^+. It is important to note that the conductivity of the materials that we reviewed is contained in a large range between 10^{-2} and 10^{-5} S/cm.

It is well known that classic liquid electrolyte formulations (i.e. organic carbonates and lithium salts, such as $LiPF_6$) provide the best ionic conductivity, compared to solid-state electrolytes, however limited to an electrochemical window up to 4.3–4.4 V vs. Li/Li^+.

On the other hand, the gap in terms of ionic conductivity values can be balanced by:

* Corresponding author.
E-mail addresses: anwar.ahniyaz@ri.se (A. Ahniyaz), imeatza@cidetec.es (I. de Meatza), akvasha@cidetec.es (A. Kvasha), ogarcia@cidetec.es (O. Garcia-Calvo), istaq.ahmed@volvo.com (I. Ahmed), mauro.sgroi@crf.it (M.F. Sgroi), mattia.giuliano@crf.it (M. Giuliano), matteo.dotoli@external.stellantis.com (M. Dotoli), aneta.dumitrescu@faam.com (M.-A. Dumitrescu), marcus.jahn@ait.ac.at (M. Jahn), ningxin.zhang@ait.ac.at (N. Zhang).

https://doi.org/10.1016/j.adapen.2021.100070
Received 6 June 2021; Received in revised form 25 September 2021; Accepted 26 September 2021
Available online 28 September 2021

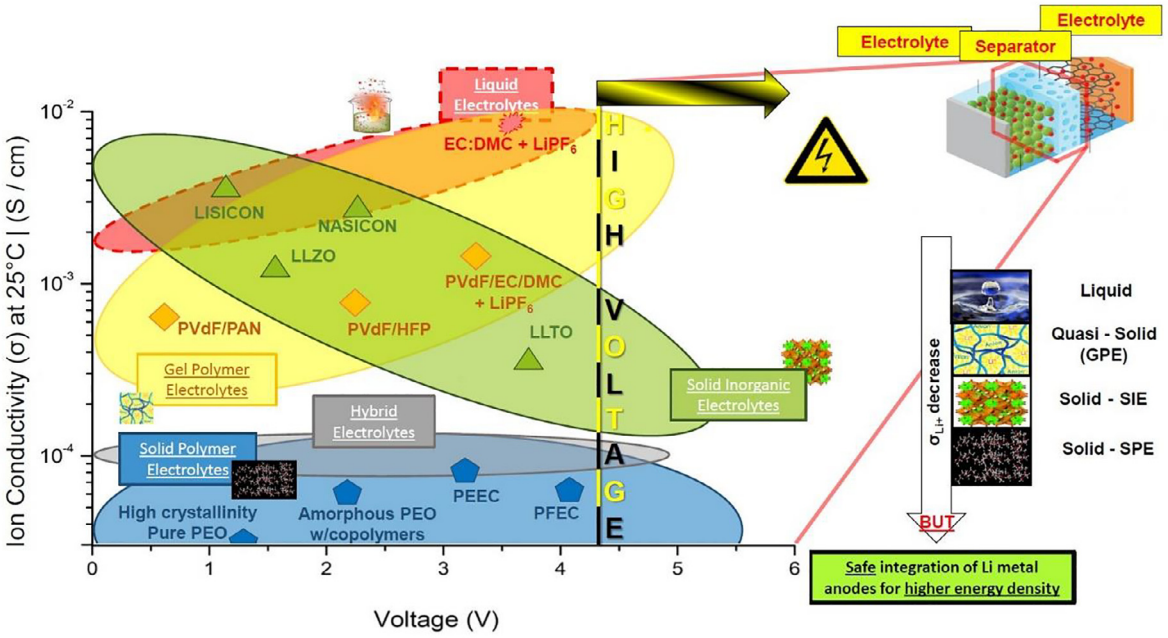

Fig. 1. The relationship between the ionic conductivity and suitable voltage windows of different electrolytes at room temperatures.

- an improvement in terms of electrochemical stability window (up to 5.5 V vs. Li/Li^+).
- better thermal stability, consequently, enhanced safety.
- elimination of separators (with a consequent cost cutting also up to 10-15% and weight & volume reduction).

1.1. Conventional lithium-ion cell

Conventional lithium ion batteries are light, compact and operate at an average discharge voltage below 4 V with a specific energy ranging between 150 Wh kg^{-1} and 300 Wh kg^{-1}. In its most conventional structure, a lithium ion battery contains a graphite anode, a cathode formed by a lithium metal oxide ($LiMO_2$) and an electrolyte consisting of a solution of a lithium salt (e.g. $LiPF_6$) in a mixed organic solvent (e.g. ethylene carbonate–dimethyl carbonate, EC–DMC) embedded in a separator felt [6].

A typical lithium ion battery configuration is shown in Fig. 2.

Normally, operate on a process (Eq. 1):

$$6C + LiMO_2 \rightleftarrows Li_xC_6 + Li_{(1-x)}MO_2,\ x \sim 0.5,\ \text{average voltage} \sim 3.7V. \quad (1)$$

Due to the complex interaction between the electrodes and electrolyte during charging and discharging process, constant decomposition and side reactions take place and this implies the consumption of active Li and electrolytes, may also results in gas evolution. These activities cause the loss of the cell capacity (initial irreversible capacity) deteriorate electrochemical performance and create safety hazards.

The separators inside lithium ion batteries experience extreme oxidizing environment on the side facing the positive electrode and extreme reducing environment on the side facing the negative electrode. The separators should be stable in these harsh conditions during long-term cycling especially at high temperature. Separators with poor oxidation resistance and thermal stability properties can lead to poor high temperature performance, safety and storage stability.

On the other hand, open circuit volatage is an important paramers in development of high powder cells.

The open-circuit voltage of a cell is the difference between the electrochemical potentials μ_A and μ_C of the anode and cathode:

$$V_{AC} = \mu_A - - \mu_C / e$$

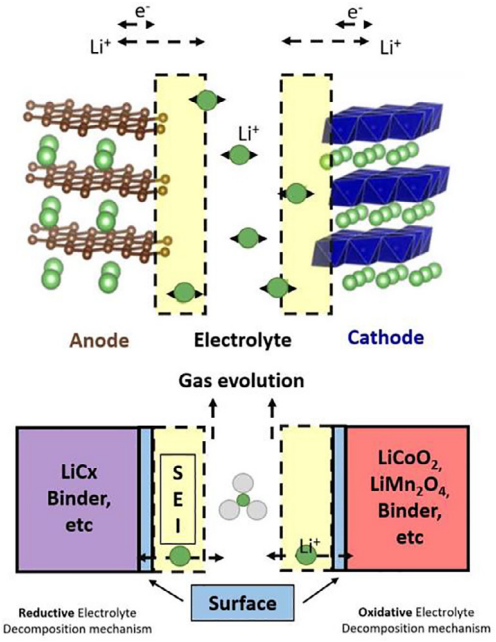

Fig. 2. Operational principle of SEI formation in a $C/LiCoO_2$ lithium ion battery.

This voltage is limited by either the “electrochemical window” of the electrolyte or by the top of the anion-p bands of the cathode. The concept of voltage window of the electrolyte is controversal in literature. According to Goodenough et al,[7] the voltage window is the energy gap between its lowest unoccupied molecular orbital (LUMO) and highest occupied molecular orbital (HOMO) of a liquid electrolyte or the bottom of the conduction band and top of the valence band of a solid electrolyte.

On the other hand, recently Peljo and Girault [8] pointed out that the concepts of HOMO and LUMO, being derived from approximated electronic structure theory of isolated molecules, are not in relation to the redox reaction occurring at the electrodes and should be avoided when talking abut the electrochemical stability of electrolytes. Accord-

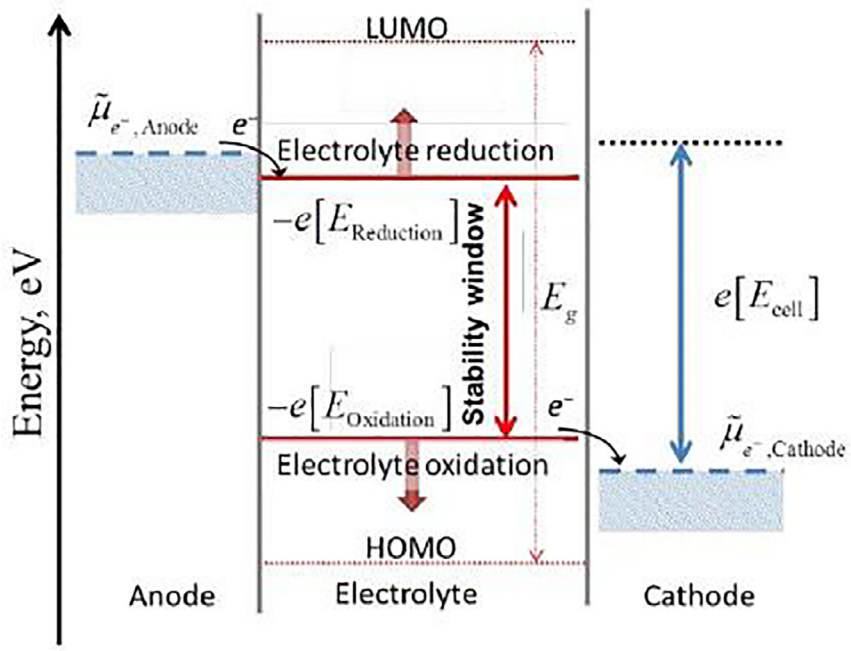

Fig. 3. Notation for the negative and positive potential limits for the electrolyte stability, and the energy levels of HOMO and LUMO (reproduced from Peljo et al. [8]).

ing to this approach it is more correct to use respectively, the potentials of electrolyte reduction (at electronegative potentials) and electrolyte oxidation (at electropositive potentials), see Fig. 3.

A value μ_A above the potential of electrolyte reduction, reduces the electrolyte unless the anode– electrolyte reaction becomes blocked by the formation of a passivating SEI layer; similarly, value of μ_C below the potential of electrolyte oxidation, oxidizes the electrolyte unless the reaction is blocked by an SEI layer. However, μ_C cannot be lowered below the top of the cathode anion-p bands, which may have an energy above the electrolyte oxidation potential. The top of the O-2p bands of the layered oxides $LiMO_2$ is ~4.0 eV below μ_A(Li), which is why oxide hosts are used as cathodes of present-day LIBs. Since the practical HOMO of the organic liquid carbonate electrolytes used in LIBs is at 4.3 eV below μ_A(Li), the voltage of the simple $LiMO_2$ layered oxides is also self-limited by the energy of the top of the O-2p bands. As a result, the $Li_{1-x}CoO_2$ originally used in the first secondary Li-ion cells evolves oxygen or inserts protons on removing Li^+ beyond x = 0.55.

The capacity of an oxide host is limited to the reversible solid–solution range of Li in the cathode host structure operating on the redox energy of a single transitionmetal cation; and where a passivating layer forms on the anode during the first charge, the capacity is further reduced by an irreversible loss of Li from the cathode in the Li+ -permeable SEI layer formed on the anode.

Therefore, formation of a stable SEI layer that allows the transport of Li^+ is critical for the cycling stability of LIBs. However, the formation of SEI layer, increases the impedance of Li^+ transfer across the anode/electrolyte interface, and its modifications/growth with successive cycling cause capacity fade of the cell.

1.2. High voltage lithium-ion cathode materials

Although the top of the O-2p bands of an oxide host can be lowered to more than 5 eV below μ_A(Li) by replacing an oxide ion with a polyanion as in $LiNiPO_4$ (see Fig. 4), investigation of these high-voltage cathodes has been limited because the organic liquid carbonate electrolytes used in the LIBs decompose at a voltage higher than 5 V. Moreover, the counter cation used to lower the top of the O-2p bands reduces the capacity unless the active redox center can accommodate two electrons without a voltage step between them.

In the case of spinel $Li[Ni_{0.5}Mn_{1.5}]O_4$ (LNMO) the states associated to different oxidation states of Ni are at the top of the O-2p bands (see Fig. 4) and this creates itinerant electrons in states with d-orbital symmetry. The itinerant property of the electrons in LNMO is associated with the good electronic conductivity of the electrode material.

Although a large number of cathodes, electrolytes and anode materials are being studied, research efforts devoted to high voltage battery materials are still limited [9–11].

For example, among the polyanion-based compounds, Li x M y (XO $_4$) z (M = metal; X = P, S,

Si, Mo, W, etc.), Li_xVOPO_4, $LiVPO_4F$, $LiMPO_4$ (M = Mn, Co, Ni) displays operating voltage above 4.8V–4.9 V vs. Li/Li^+ [12–15].

The most common material in this class is Li_xFePO_4 (LFP), and widely used olivine type of cathode with a theoretical capacity of 170 mAh/g. However, LFP has a low voltage output 3,2-3,5 V vs Li/Li^+. In order to increase the energy density of the olivine type of materials, researchers developed LiCoPO4 which can be cycled at 4,8 V vs. Li/Li^+ [13,16–20].

$LiCoPO_4$, is characterized by a flat voltage profile, and a high theoretical capacity comparable to that of LFP. However, $LiCoPO_4$ is a very unstable cathode material in $LiPF_6$-containing electrolytes [21,22] since the de-lithiated (charged) state is prone to a nucleophilic attack of F^- anions on the P atoms, leading to the degradation of the material [23].

Among the spinel compounds, LNMOs, delivers a specific energy density equivalent to 650 W h kg^{-1}, which is the highest among the commercially available cathode materials such as $LiCoO_2$ (518 W h kg^{-1}), $LiMn_2O_4$ (400 W h kg^{-1}), $LiCo_{1/3}Ni_{1/3}Mn_{1/3}O_2$ (576 W h kg^{-1}) and $LiFePO_4$ (400 W h kg^{-1}).[24]

There is a new challenges to develop a suitable electrolyte for high voltage cathode materials, proven to work with cathode 3,7 V vs. Li/Li^+ or higher (LCO, NMC and up) exluding LFP. Therefore, main focus of this review is to highlight most recent developments on high voltage electrolyes, especially these electrolytes suitable for lithium ions and lithium metal batteries.

2. High voltage lithium-ion cell electrolytes

Classification of electrolytes for high voltage batteries

Fig. 5 depicts a very general classification of electrolytes. In general, there are three main classes of electrolytes: solid polymer electrolytes (SPE), solid inorganic electrolyte (SIE) and liquid electrolytes and component (LEC). Note that it is difficult to fulfill all requirements within

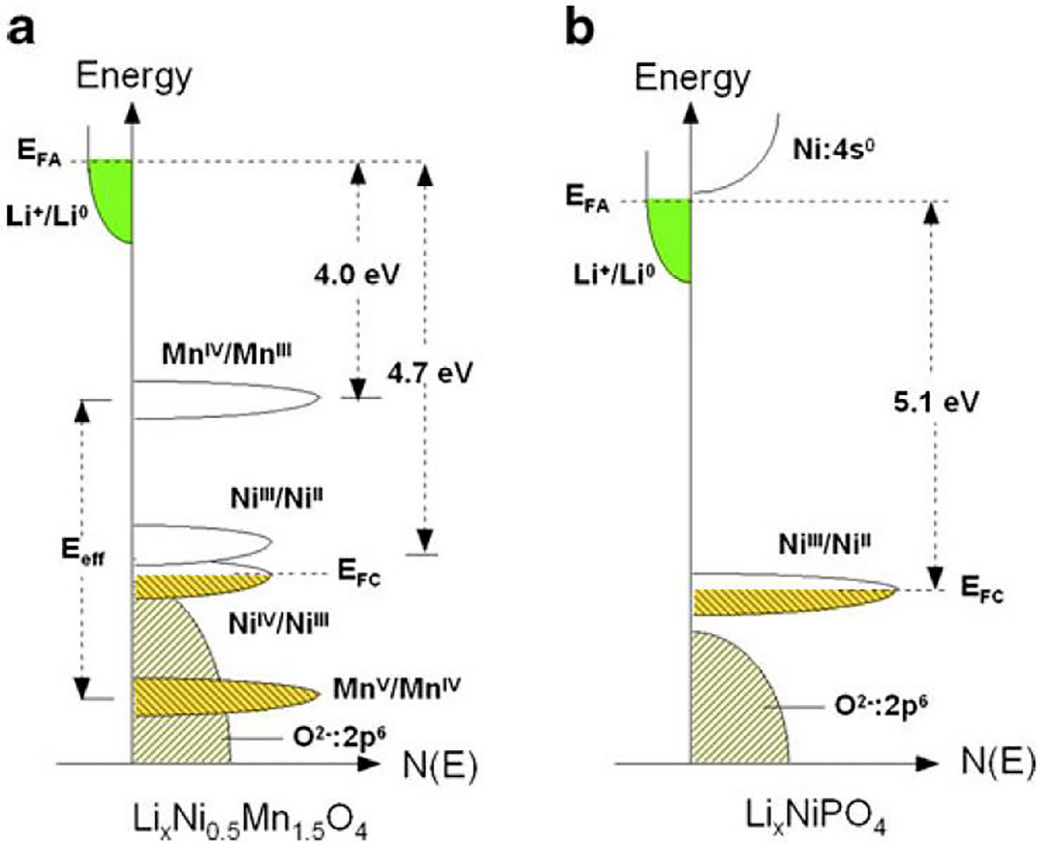

Fig. 4. *A* schematic density of states and Fermi energies for a LixNi0.5Mn1.5O4 spinel and b LixNiPO4 olivine cathodes. The origin of energies is chosen at the Fermi energy of lithium metal, (reproduced from Mauger and Julien) [177].

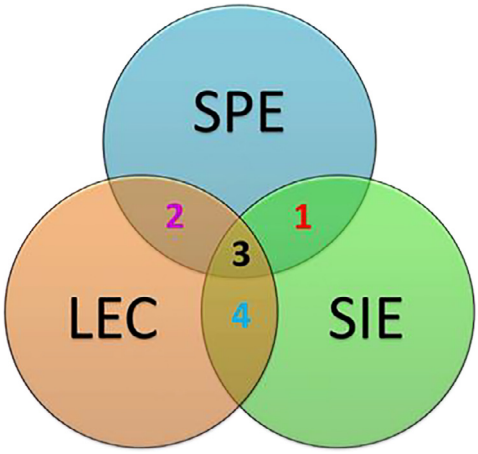

Fig. 5. Venn diagram of main electrolyte types: SPE – solid polymer electrolyte, SIE – solid inorganic electrolyte, LEC – liquid electrolytes and components (ionic liquids, plasticizers etc.). Overlapping areas: 1 – hybrid electrolytes, 2 – gel polymer electrolytes, 3 – hybrid gel polymer electrolytes, 4 – pseudo/quasi solid electrolytes.

a certain electrolyte type, therefore, many electrolytes such as hybrid electrolytes, gel polymer electrolytes, hybrid gel polymer electrolytes and pseudo/quasi solid electrolytes with interesting physical-chemical and electrochemical properties have been discovered in the four overlapping areas showed in Fig. 5.

Moreover, safety requirements greatly restrict the possible choices of candidate materials: commercial cells must respect strict standards in terms of thermal stability and presence of dangerous substances. For this reason, along with the development of thermally and electrochemically stable electrolytes, it is important to develop separators that fit to operate in a wide temperature range.

2.1. Liquid electrolytes

Liquid electrolytes for Li-ion batteries consist of a mixture of a lithium salt solvated in a mixture of solvents (Table 1) [25–27].

Generally, liquid electrolytes require two main features: high dielectric constant and low viscosity, hard to find both parameters on a single solvent. To gain both salt solvation and ions transport, the common strategy consists of mixing different solvent types.

In this framework, esters (linear and cyclic carbonates) are among the most used solvent, because of their resistance to anodic decomposition at cathode surfaces and limiting their higher cathodic decomposition potential by forming a stable SEI layer on the anode.

Ethylene carbonate (EC) is the most suitable solvent for SEI formation but because at room temperature it is a solid, it must be used together with acyclic carbonates (DMC, DEC, EMC). By mixing these solvents, it has been possible to reach the ionic conductivity in the range of 5–10 mS/cm at room temperature (RT), with a range of thermal stability between -30 to 60 °C.

The panorama of electrolytes includes nitriles as one of the most promising materials with ion conductivities higher than 30 mS at RT, even if limited by a narrow electrochemical stability window. One of the most used strategies is the introduction of fluorine atoms into solvent molecules that improves solvent polarity, oxidation durability, liquid temperature range and no flammability, which would result in better cell performances.

Table 1
Liquid solvents.

Solvent	Melting Point (°C)	Boiling Point (°C)	Homo (eV)	Lumo (eV)	Dielectric constant (25°C)	Viscosity (mPa, 25°C)	Ref.
Acyclic Carbonates							
DMC	4.6	91	-6.3	0.25	3.11	0.59	[178–180]
EMC	-53	110	-7.67	1.17	3	0.65	[180,181]
DEC	-74	126	-7.67	1.24	2.81	0.75	[181]
Cyclic Carbonates							
EC	36	238	-8.02	1.07	90 (at 40°C)	1.9 (at 40°C)	[180]
PC	-49	242	-7.9	1.01	69	2.5	[180]
2,3-BC	34	243	-7.9	1.06	57	2.8	[182]
Sulfones							
Tetramethylene sulfone (TMS)	27	285	-	-	43	10	[180,183,184]
Ethylmethyl sulfone (EMS)	33	-	0.90/0.72	11.87/11.66	57.5 (at 30°C)	High	[180]
Nitriles							
Acetonitriles (ACN)	-44	82	-9.9/-8.1	0.0/-1.2	36.6	0.37	[180,185]

Table 2
Salts for liquid electrolytes.

Salt	Melting Point (°C)	T Decomp. in solution (°C)	σ (mS/cm) at 25°C in EC/DMC	Electrochemical Stability	Al Corrosion	Ref.
$LiPF_6$	293	80	10.7	up to 4.5	No	[186]
$LiBF_4$	200	Over 100	4.9	up to 4.5	No	[186]
$LiAsF_6$	340	Over 100	11.1	up to 4.5	No	[186]
$LiClO_4$	236	Over 100	8.4	up to 5.1	No	[186]
LiTf	Over 300	Over 100	-	-	Yes	[186]
LiBOB	-	Over 300	8-9	up to 4.2	No	[187]
LTOP	No melting	150-190	8.0	up to 5.5	-	[28]
LiFAB	-	-	7.6	up to 4.2	No	[188]

Even if less common, also linear and acyclic carboxylates, borates, aluminates, sulfones and sulfoxides, phosphorus and silicon-based solvents and ethers are currently under investigation.

Among salts (Table 2), $LiPF_6$ is nowadays the most common in commercial cells, due to the combination of many favorable properties. However, it has also drawbacks, especially on chemical and thermal instability, limiting the performance of the system while in applications. In this perspective, the scientific community is trying to overcome these limitations by the introducing new salts, with the aim of gaining both thermal and high voltage window stability.

In this sense, lithium bis(oxalate) borate (LiBOB) offers good performance at high temperatures, but it does not support high voltage window stability (higher than 4.2 V vs. Li/Li^+).

Another approach uses lithium tetra fluoro(oxalate) phosphate (LTFOP), selected among phosphate salts [28]. It combines $LiPF_6$ and LiBOB peculiarities of chemical/thermal stabilities at high temperatures.

Among borate salts, $LiBF_4$, it has lower solubility in carbonates because of its high viscosity, thus exhibit low ion conductivity.

Apart from $LiBF_4$, lithium pentafluoroethyl trifluoroborate (LiFAB), shows lower conductivity at 25 °C and above but shows higher conductivity at lower temperatures (less than -10 °C).

In addition, hybridized forms are investigated i.e. lithium difluoro (oxalate) borate (LiDBOB). One of the latest approaches were observed in implementing imides salts. The first that had been introduced was lithium bis(trifluoromethanesulfonyl)imide(LiTFSI), followed by lithium (fluorosulfonyl)(nonaflurobutanesulfonyl)imide(LiFNFSI). Despite some limitations related to aluminum corrosion (mostly below 4 V vs. Li/Li^+) they maintain good stability up to 180 °C.

2.2. Gel electrolytes

Gel electrolytes are considered as an alternative to all solid-state electrolytes. These materials have properties in common with both liquid and solid electrolytes, providing a hybrid solution. Gels are prepared by introducing a liquid phase (liquid electrolyte or ionic liquid) into a polymer matrix (Fig. 6). In this approach, electrolyte materials have mechanical properties similar to plastic solids and, simultaneously, ion transport properties closer to liquid electrolytes. Thus, battery performance is generally improved in terms of operating temperature, C-rate capability and cyclability in comparison with SPEs. Moreover, these materials may be used in a combination with high voltage cathode materials, due to their wider electrochemical stability window comparing to competitors.

A list of different types of gel electrolytes, gel polymer electrolytes (GPEs) and ionic gel polymer electrolytes (IGPEs) analyzed in this work is presented in Table 3.

2.2.1. Gel polymer electrolytes (GPEs)

Most common polymer materials for gel electrolytes is, poly(vinylidene difluoride) (PVdF), and it is studied widely due to its attractive characteristics such as good affinity to liquid electrolyte solutions, good mechanical and electrochemical stability and high dielectric constant [29]. However, the mobility of lithium ions is hindered by the crystalline part of PVdF, but this may be decreased by different approaches such as using poly(vinylidenefluoride-*co*-hexafluoropropylene) copolymers (PVdF–HFP) [30], incorporating nanometric fillers (e.g. SiO_2) [31] or blending with a different polymeric material (e.g. polyacrylonitrile) [32].

In 2000, Periasamy et al. [33] reported a GPE based on PVdF, a $LiBF_4$ salt and a mixture 1:1 (vol.%) of ethylene carbonate (EC) and propylene carbonate (PC), which possesses high ionic conductivity at room temperature (6.4 mS/cm). That electrolyte was tested in a $Li/LiCoO_2$ cell providing a good voltage performance and a coulombic efficiency of ~85% after 25 cycles. Later, Zhang et al. [34] prepared by solvent-casting method a polymer membrane film composed of PVdF and salicylic acid as a foaming agent. Afterwards, a heat treatment and the addition of liquid electrolyte led to PVdF-based porous GPE with an ionic conductivity of 4.8 mS/cm at room temperature. The corresponding $LiCoO_2$/GPE/Li cell provided slow capacity fading, with only 10% of capacity loss after 100 cycles. More recently, Lombardo et al. [35] published results about a high voltage cell made by in-situ polymerization of a PVdF/EC:dimethyl carbonate(DMC) (1:1 vol.%) precursor. The as-prepared polymer membrane was impregnated with a solution of 1M $LiPF_6$ in EC: DMC (1:1 vol.%) gaining an ionic conductivity of 3 mS/cm at ambient temperature. The in-situ polymerized $LiNi_{0.5}Mn_{1.5}O_4$/GPE/Li cell was tested a C/5 rate within the voltage

Table 3
Main features of the high voltage gel polymer electrolytes and corresponding batteries.

Gel Polymer Electrolyte			Battery						Ref
Formulation	σ at RT,mS/cm	E_{ox}V vs. Li/Li+	Negative electrode	Positiveelectrode	Cycling conditions	$Q_{dis1,}$ mAh/g	Capacityretention Cycle	%	
PVdF/PAN + 1M $LiClO_4$ in PC	7.8	5.1	Li	$LiCoO_2$	2.8 - 4.25 V, 0.1C	120.4	150	93	[32]
PVdF, $LiBF_4$ in EC/PC (1:1)	6.4	-	Li	$LiCoO_2$	3.0 – 4.25 V charge: 0.075 mA/cm^2 discharge: 0.065 mA/cm^2	142.5	25	89	[33]
PVdF/ salicylic acid +1M $LiPF_6$ in EC/DMC (1:1)	4.8	-	Li	$LiCoO_2$	3.0 – 4.3 V	~140	100	90	[189]
PVdF/EC:DMC (1:1) +1M $LiPF_6$ in EC/DMC (1:1)	3.0	5.0	Li	$LiNi_{0.5}Mn_{1.5}O_4$	3.5 – 5.0 V, 0.2C	~120	60	>99	[35]
PVdF/ PEGDA + 1M $LiPF_6$ in EC/DMC (1:1)	4.0	4.7	Li	$LiCoO_2$	3.0 – 4.2 V, C/3	~120	50	>92	[36]
PVdF/PLS-20 + 1M $LiPF_6$ in EC/PC/DMC (1:1:1)	4.49	4.95	Li	$LiCoO_2$	2.5 – 4.4 V, 0.1C	175.6	50	83	[38]
PvdF/SiO_2-g-P(MMA-co-HEMA)+1M $LiClO_4$ in PC	2,63	4,8	Li	LiMn2O4	2,0-4,0, 0,2C	120	50	90	[39]
PVdF-HFP/ PEG/ PEGDMEA + 1M $LiPF_6$ in EC/DEC (1:1)	1.06	5.0	meso-carbon	$LiCoO_2$	2.7 – 4.2 V, 0.5C	120	50	85	[40]
PVdF-10CTFE + 1M $LiPF_6$ in EC/DMC (1:1)	2.0	-	Sn–C	$LiNi_{0.5}Mn_{1.5}O_4$	3.0 – 4.9 V, C/3	120	N/A	N/A	[41]
Cellulose/PVdF-HFP + 1M $LiPF_6$ in EC/DMC (1:1)	1.4	5.3	graphite	$LiCoO_2$	2.75 – 4.2 V, 0.5C	118	100	83	[42]
PVDF-HFP-PPC + 1M $LiPF_6$ in EC/DEC (1:1)	1.18	4.8	Li	$LiFe_{0.2}Mn_{0.8}PO_4$	2.5 – 4.4 V, 0.2C	155.5	100	89.8	[43]
AMS + 1M $LiBF_4$ in EC/DMC (1:1)	2.3	4.2	Li	$LiNi_{0.5}Co_{0.5}O_2$	3.0 – 4.2 V, 0.1C	156	50	>80	[44]
PPC + 1M LiDFOB in PC	0.11	5.0	Li	$LiNi_{0.5}Mn_{1.5}O_4$	3.5 – 5.0 V, 0.5C	~120	100	91.3	[45]
P(MVE-MA) + 1M LiDFOB in PC	1.6	5.2	Li	$LiCoO_2$	2.75 – 4.45 V, 1C (60°C)	178.4	700	85	[46]
TPU + 50 wt.% PQ + 1 M $LiPF_6$ in EC/DMC (1:1, w/w)	3,78	-	Li	LiNi0.6Mn0.2Co0.2O2	3,0-4,5, 0,5	193	100		[47]
PMMA + 1M $LiPF_6$ in EC/DEC (1:1)	~ 1.0	4.2	graphite	$LiNi_{0.8}Co_{0.2}O_2$	3.0 – 4.2 V, 0.06 mA/cm^2	145	20	85	[48]
Cellulose/PVCA-LiDFOB	0.02	5.0	Li	$LiCoO_2$	2.5 – 4.3 V, 0.1C	146	150	84.2	[49]
PVCA + 1M LiDFOB in EC/DEC (1:1)	0.56	5.0	graphite	$LiFe_{0.2}Mn_{0.8}PO_4$ (coin cell) $LiNi_{0.6}Co_{0.2}Mn_{0.2}O_2$ (pouch cell)	2.5 – 4.35 V, 0.1 C	137	1000	88.7	[50]
PECA + 1M $LiPF_6$ in EC/DEC	2.7	4.8	Li	$LiNi_{0.5}Mn_{1.5}O_4$	2.5 – 4.0 V, 1C	140	100	93	[51]
IPN-PDEC + 1M $LiPF_6$ in EC/DMC	0.16	4.5	Li	$LiFe_{0.2}Mn_{0.8}PO_4$	2.5 – 4.35 V, 0.1C	140	100	96	[52]
PETEA + 1M $LiPF_6$ in EC/DEC/DMC (1:1:1)	8.46	4.5	graphite	$LiNi_{0.8}Co_{0.15}Al_{0.05}O_2$	2.75 – 4.2 V, 0.5C/1C	2.3 (Ah)	280	86.4	[53]
Cross-linking PAMM + 1M $LiPF_6$ in EC/DEC (1:1)	0.68	5.0	Li $Li_4Ti_5O_{12}$	$LiNi_{0.5}Mn_{1.5}O_4$ $LiNi_{0.5}Mn_{1.5}O_4$	3.5 – 5.0 V, 0.1C	132	500	89.5	[54]
BMImNfO/LiNfO/PVdF-HFP	3.7	4.9	Li	$LiCoO_2$ (Swagelok)	3.0 – 4.2 V, C/4	138.1	30	91	[54]
EMImNfO/LiNfO/PVdF-HFP	0.1	5.4	Li	$LiCoO_2$	2.9 – 4.2 V, 0.1C	164	45	98	[56]
EMImDFOB/LiDFOB/PVdF-HFP	0.3	4.46	Li	$LiCoO_2$	3.0 – 4.2 V, 0.1C	148.4	100	81	[57]
EMIMFSI/LiTFSI/PEO	0.83	5.0	Li	$LiNi_{0.80}Co_{0.15}Al_{0.05}O_2$	3.2 – 4.2 V, 0.1C	175	200	>99	[58]
PVdF-HFP + 20wt.% LiTFSI + 70 wt.% PYR13FSI	3,9	4,3	Li	Li_2CuO_2@$LiNi_{0.33}Mn_{0.33}Co_{0.33}O_2$	2,4-4,2, 1C	130	100	69	[59]
[P(VdF-HFP)+PMMA] + 20wt.% LiTFSI + 70 wt.% EMIMTFSI	2,5	4,2	Li	$Li_{1.2}Ni_{0.6}Mn_{0.1}Co_{0.1}O_2$	2,4-4,2, 0,1C	166	50	67	[59]

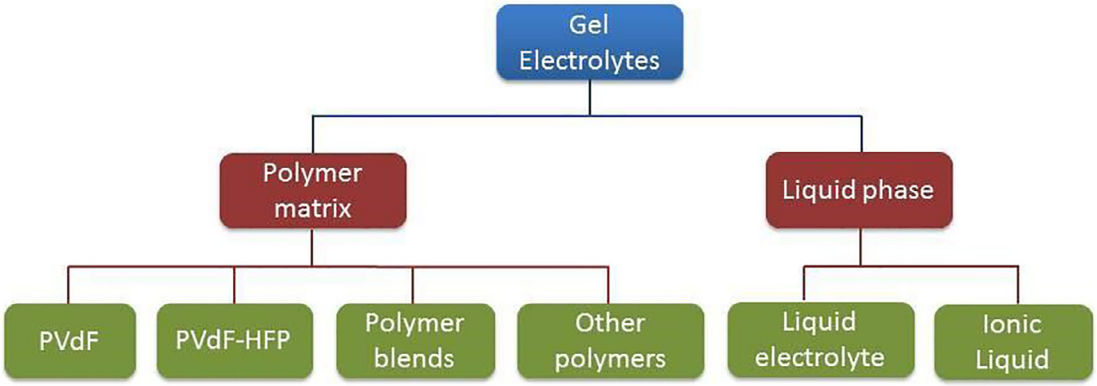

Fig. 6. Main components of gel electrolytes.

range 3.5–5.0 V. This cell displayed a reversible capacity of 120 mAh/g with relatively low efficiency during the initial 10 cycles, most likely due to solid electrolyte interface (SEI) film formation at the lithium electrode surface. During the following cycles the stabilization of the SEI layer prevents further electrolyte decomposition and the cell efficiency values increased, with remarkable reversibility and high-capacity retention.

In accordance with already mentioned strategies to reduce the crystallinity of PVdF polymer, Song and co-authors [36] reported the characterization of UV-cured PEGDA/PVdF blend gel polymer electrolytes and their application in rechargeable lithium batteries. PEGDA/PVdF (5/5) blend, containing EC-based liquid electrolyte, had an ionic conductivity of 4 mS/cm at room temperature and an electrochemical stability of 4.7 V vs Li/Li^+. The electrochemical data of Li|(PEGDA/PVdF)|$LiCoO_2$ cell at C/3 rate show very good cyclability for a PEGDA/PVdF (5/5) blend electrolyte when cycled between 3.0 and 4.2 V. The discharge capacity decreases more slowly during cycling and this cell retains more than 92% of the initial discharge capacity after 50 cycles. Later, Golapan et al. [37] synthesized PVdF-PAN electrospun fibrous membranes, converted them into GPEs by soaking in 1M $LiClO_4$-PC solution and tested them in $LiCoO_2$/GPE/Li cells at 0.1 C rate between 2.8 and 4.25 V. The most promising electrolyte, i.e. PVdF/PAN (75:25 by weight), exhibited a high ionic conductivity of about 7.8 mS/cm at 25 °C, an anodic stability up to 5.1 V versus Li and a remarkable capacity retention (93% after 150 cycles). In 2014, hybrid microporous gel polymer electrolytes based on PVdF/polyurethane lithium salt (PLS) were prepared by Xing et al. [38]. These materials were composed of three components: (I) hybrid polymer matrix, (II) liquid electrolyte stored in the pores of the polymer membrane and (III) gel polymer electrolyte formed by swelling of liquid electrolyte in the membrane. The electrochemical performance of these GPEs was tested in $LiCoO_2$/GPE/Li cells at 0.1 C between 2.4 and 4.5 V. Thus, the initial discharge capacity with PVdF/PLS (80:20 by weight) was 175.6 mAh/g, with a coulombic efficiency of 97% and a capacity retention of 83%, both after 50 cycles.

More recently, the group of Javanbakht et al. [39] reported PVDF-based nanocomposite GPE containing SiO_2-g-p(methyl methacrylate-co-hydroxyl ethyl methacrylate) (PMMA-co-HEMA) organic-inorganic hybrid nanoparticles, combined with 1 M $LiClO_4$ in PC. The ionic conductivity of the prepared GPE was 2.63 mS/cm at room temperature and their electrochemical stability window was established to be as high as 4.8 V (vs. Li/Li^+). In addition, $LiMn_2O_4$/Li cell assembled with this nanocomposite GPE exhibits stable electrochemical performance up to 50 cycles at 25 ^{0}C and 0.2 C, with a discharge capacity retention of 90%.

Among the different polymer matrices suitable for GPEs, PVdF-co-HFP is considered as a good polymer host because of its lower crystallinity than the corresponding homopolymer, high electrochemical stability and ability to dissolve lithium salts. In this aspect, Cheng et al. [40] reported the preparation and characterization of chemically cross-linked porous gel polymer electrolytes based on PVdF-HFP/PEG/PEGDMEA blends. The optimized PVdF–HFP/PEG/PEGDMA (5/3/2 wt.%) electrolyte containing 1M $LiPF_6$/EC–diethyl carbonate (DEC) (electrolyte uptake: 98%) showed in a full cell with carbon anode and $LiCoO_2$ cathode high ionic conductivity (1.06 mS/cm), wide electrochemical window (5 V vs. Li/Li^+), moderate cyclability (50 cycles at C/2) and good rate capability (at 2 C the cell delivered the 80% of the nominal capacity. Later, an electrospun gel polymer electrolyte (EGPE) based on poly(vinylidenefluoride-co-chlorotrifluoroethylene) copolymer (PVdF:CTFE 90:10 molar ratio) and battery grade electrolyte LP30, 1M $LiPF_6$ – EC:DMC (1: 1 w/w), was reported by Croce et al.[41]. Complete lithium-ion cells were assembled using nanostructured Sn–C composite anode, $LiNi_{0.5}Mn_{1.5}O_4$ cathode and EGPE-PVdF-CTFE electrolyte. The lithium-ion cells were cycled at various C-rates and within a 3.0–4.9 V voltage range, delivering a capacity of 120 mAh/g at C/3 rate, which corresponds to a specific energy as high as 480 Wh/kg. In 2013, Zhang et al. [42] developed a renewable cellulose-based gel electrolyte made by electrospinning followed by dip-coating in a solution of PVdF-HFP/acetone (2/98 wt.%), obtaining a thermally and electrochemically stable GPE, with high ionic conductivity at room temperature. Moreover, this electrolyte was tested in a coin cell with a $LiCoO_2$ cathode and a natural graphite anode, after activating it by filling with 1M $LiPF_6$/PC: DMC(1:1) liquid electrolyte. Thus, the cell with the cellulose/PVdF-HFP composite separator exhibited acceptable cyclability, higher discharge capacity at 0.5 C (118 mAh/g) and much better rate capability at various rates as compared to the PP separator. Recently, Liang et al. [43] prepared a GPE based on blending poly(propylene carbonate) (PPC) into PVdF-HFP, with the aim of improving the electrochemical performance of solid-state lithium ion batteries (LIBs). This GPE was obtained by immersing a dry membrane of PVdF-HFP-PPC (1:1 mass ratio) into the liquid electrolyte 1M $LiPF_6$ in EC: DEC (1:1 vol.). They demonstrated that the electrochemical performance of PVdF-HFP based electrolyte improved by blending the strong polar carbonyl groups of PPC into the PVdF-HFP polymer matrix. Thus, the corresponding GPE exhibits high ionic conductivity (1.18 mS/cm) and transference number (t_{Li+} = 0.47), and electrochemical window up to 4.8 V (vs. Li/Li^+). The Li/$LiFe_{0.2}Mn_{0.8}PO_4$ cell with the blending GPE delivered a high discharge capacity of 162.3, 155.5 and 130.1 mAh/g at 0.1, 0.2 and 0.5 C charge-discharge rates, respectively. Furthermore, the cycling performance of Li/GPE/$LiFe_{0.2}Mn_{0.8}PO_4$ cell in applied voltage range of 2.5–4.4 V at 0.2 C showed a capacity retention of 89.8% after 100 cycles and nearly 100% coulombic efficiency.

On the other hand, it is highly desirable to develop alternative polymer matrices to PVdF-HFP at a lower cost, environmental benignity, wider electrochemical window as well as easy fabrication. In this context, Kim and Sun [44] reported the synthesis of acrylonitrile-methyl

methacrylate-styrene (AMS) terpolymers and the preparation of AMS-based gel polymer electrolytes using binary plasticizing solvents consisting of EC/DMC (1:1) or EC/ γ -butyrolactone (γ-BL) (1:1). Although EC/ γ-BL-based polymer electrolyte exhibited higher ionic conductivity ($5.3\bullet10^{-3}$ S/cm) than EC/DMC-based polymer ($2.3\bullet10^{-3}$ S/cm), the poor interfacial properties between lithium and the electrolyte limit cycling performance of the Li/SPE/$LiNi_{0.5}Co_{0.5}O_2$ cell. Thus, the cell which contains the EC/DMC mixture had an initial capacity of 156 mAh/g at 0.1C in the voltage range of 3.0–4.2 V. It also showed an attractive discharge capacity of 116 mAh/g at 2C rate.

Among the most investigated polymer matrices, poly(propylene carbonate) (PPC) has attracted increasing attention as a promising polymer matrix for LIBs owing to its low cost and biodegradability. Zhao [45] developed a sustainable and rigid-flexible coupling cellulose-supported PPC polymer electrolyte for $LiNi_{0.5}Mn_{1.5}O_4$-based batteries. The polymer membrane was prepared by solvent casting and submerged in the liquid electrolyte for 12 h to obtain the composite PPC-GPE (PPC membrane in PC/Lithium oxalyldifluroborate (LiODFB)). The corresponding Li/PPC-GPE/$LiNi_{0.5}Mn_{1.5}O_4$ cell was tested between 3.5 and 5 V at a constant charge–discharge current density (0.5C = 200 $mA\bullet cm^{-2}$). $LiNi_{0.5}Mn_{1.5}O_4$/Li cell with PPC-GPE maintained 91.3% of the initial discharge capacity after 100 cycles at 0.5 C. Moreover, rate capability of this cell was studied from 0.5 C to 5 C, at C rates of 0.5, 1, 2, 3 and 5 C, providing the discharge capacity of 109.1, 100.1, 89.3, 80.1 and 66.5 mAh/g, respectively. More recently, the same research group [46] reported a cellulose-supported poly (methyl vinyl ether-*alt*-maleic anhydride) (P(MVE-MA)) based GPE (abbreviated as PMM-CPE), with a wide electrochemical window (> 5.2 V versus Li/Li^+ LRE) and high ionic conductivity at different temperatures from 25 °C to 80 °C (~10^{-3} S/cm at RT). Furthermore, PMM-CPE possessed a high lithium ion transference number ($t_{Li}{}^+ = 0.54$), which is beneficial for increasing the rate performance and decrease the polarization of cells. Also, this material was tested in a 4.45 V $LiCoO_2$/Li cell, obtaining superior capacity retention (85% after 700 cycles) and excellent rate capability (15C) even at 60 °C. This exceptional battery performance was attributed to a favorable protection film on the $LiCoO_2$ cathode and a stable SEI film on the Li anode. More recently, Ye and co-authors [47] developed polymer-filler-reinforced membranes composed of lithiophilic polyacenequinone (PQ) as filler and thermoplastic polyurethane (TPU) as polymer electrolyte matrix. Later, corresponding GPE were formed by immersing as-prepared polymer membranes in 1 M $LiPF_6$ electrolyte (EC/DMC, 1:1, w/w). Three different PQ filler mass percentages of 30, 50 and 80% were tried in order to optimize the GPE formulation. The GPE with 50 wt.% of PQ filler showed the best ionic conductivity result (3.78 mS/cm @ RT) and a high lithium-ion transfer number ($t_{Li+} = 0.74$), which could be attributed to the enlarged amorphous region induced from the addition of PQ filler and the decreased hopping distance of Li^+ due to the sufficient carbonyl groups of PQ. Finally, the electrochemical performance of this GPE (50 wt.% PQ filler) was then examined in a half-cell system by employing NCM622 as cathode, delivering a high specific capacity of 145 mAh/g and a stable coulombic efficiency approaching 99% after 100 cycles at 0.5C rate.

In general, polymer electrolytes are usually prepared by a solvent casting method employing toxic solvents and long processes. As an alternative, in-situ polymerization (ISP) has been a promising strategy to easily achieve polymer electrolytes directly inside the batteries. In this method, a precursor solution of monomer/s, plasticizer, lithium salt and initiator is injected into the battery package, followed by in-situ polymerization under proper conditions, such as thermal initiation or γ-ray irradiation. Therefore, in-situ generated polymer electrolytes have an excellent interfacial compatibility with cathode and anode, which contributes to reduce the interfacial resistance of the lithium cells.

In this context, Amine and co-authors [48] reported the preparation of a poly(methyl methacrylate) (PMMA) a liquid precursor and the batteries were assembled by the relatively simple technology used for conventional liquid electrolyte lithium ion batteries, followed by γ-ray irradiation of the assembled cells to obtain gel polymer type cells. The full cell $LiNi_{0.8}Co_{0.2}O_2$/PMMA-GPE/graphite was tested at a current density of 0.06 $mA\bullet cm^{-2}$ in a voltage range between 3.0 and 4.2 V, showing good cycling performance after the first charge–discharge cycle, although its specific capacity is a little lower than that of a liquid-electrolyte-based cell at the same current density. Later, Chai et al. [49] showed a cellulose-supported poly(vinyl carbonate) based solid polymer electrolyte (PVCA-SPE) generated via in-situ polymerization process which possessed moderate ionic conductivity ($2.23\bullet10^{-5}$ $S\bullet cm^{-1}$ at 25 °C), high Li^+ transference number ($t_{Li+} = 0.57$) and wide electrochemical window (5.0 V at 25 °C and 4.5 V at 50 °C). Moreover, the electrochemical performance of the PVCA-SPE based lithium batteries was evaluated by using high voltage $LiCoO_2$ (4.3 V) as the cathode and Li metal as the anode, with the voltage range of 2.5–4.3 V at different C-rates varied from 0.1 to 0.5 C. Thus, they obtained 146 mAh/g at 0.1C, 114 mAh/g at 0.2 C and 73 mAh/g at 0.5 C. In addition to this, they evaluated the safety characteristics of pouch type cells using PVCA-SPE by nail penetration test, keeping a good shape without any flame, explosion, neither short circuit. More recently, Chai et al. [50] reported a similar material prepared by in-situ polymerizing a mixture of solutions of 1M LiDFOB in vinylene carbonate (VC) and 1M LiDFOB in ethylene carbonate/dimethyl carbonate (EC/DEC, 1/1 by volume). First of all, electrochemical properties of this material were evaluated in order to ensure acceptable ionic conductivity, transference number and electrochemical stability values. Afterwards, this GPE was tested in high voltage cells with different configurations; $LiFe_{0.2}Mn_{0.8}PO_4$/graphite in 2032-type coin cell, and $LiNi_{0.6}Co_{0.2}Mn_{0.2}O_2$/graphite in pouch cell. In the case of coin cells, they obtained a discharge capacity of 137 mAh/g at a current density of 0.1 C, with a 88.7% capacity retention and nearly 100% columbic efficiency over 1000 cycles at a current density of 1 C. On the other hand, a 30 mAh Li-ion pouch cell displayed stable charging/discharging profiles at a rate of 0.1 C and could light a LED lamp in a normal state, in a bended state and even after being cut a half away.

Continuing the research on in-situ polymerized GPEs, the same group [51] prepared a poly(ethyl cyanoacrylate) (PECA) based GPE electrolyte by in-situ anionic polymerization method. The PECA-GPE electrolyte possessed excellent ionic conductivity (2.7 mS/cm at room temperature) and high transference number ($t_{Li+} = 0.45$). A $LiNi_{0.5}Co_{1.5}O_4$/PECA-GPE/Li cell was tested at different C-rates showing reversible capacities about 155, 145, 140, 120, and 110 mAh/g at 0.2, 0.5, 1 (0.8 mA/cm^2) 2, and 3 C discharge rates, respectively. Furthermore, excellent cycling behavior was also achieved with a discharge capacity of 122 $mAh\bullet g^{-1}$ at 1C (0.6 mA/cm^2) after 100 cycles. Additionally, poly(diethylene glycol carbonate)dimethacrylate (PDEC-DMA) based interpenetrated GPE (IPN-PDEC) was also developed by Liu et al. [52]. In this work, they synthesized first the PDEC-DMA macromonomer followed by the preparation of gel electrolyte precursor and injected it directly into a 2032-type battery. After characterizing the electrochemical properties of this GPE, they assembled $LiFe_{0.2}Mn_{0.8}PO_4$/IPN-PDEC/Li cells and tested them in a voltage range of 2.5–4.35 V, using cellulose separator to avoid internal short-circuit. C-rate capability of $LiFe_{0.2}Mn_{0.8}PO_4$/IPN-PDEC–$LiDFOB_{15}$/Li cell was tested at 25 °C at different C-rates (0.05 C, 0.1 C and 0.2 C). Moreover, the cycling performance of this cell was evaluated at 0.1 C, delivering a discharge capacity of 140 mAh/g after 100 cycles, which corresponds to 96% capacity retention. Later, Li [53] reported a high voltage Li-ion battery also obtained by in-situ polymerization. The GPE precursor was prepared by mixing pentaerythritol tetra acrylate (PETEA, 1.5 wt.%), α,α'-azoisobutyronitrile (AIBN, 0.1 wt.%) and 1M $LiPF_6$ in EC/DEC/EMC (1:1:1 vol.%). Four types of batteries, that is, $LiNi_{0.8}Co_{0.15}Al_{0.05}O_2$ (NCA)/LE/graphite, NCA/liquid electrolyte/(graphite–Si/C), NCA/PETEA-based GPE/graphite, and NCA/PETEA-based GPE/(graphite–Si/C), were assembled. The energy densities of these 2 Ah pouch cells were 210, 215, 225 and 228 Wh/kg, respectively. The most promising cell, with configuration NCA/PETEA-

based GPE/graphite, delivered 2.3 Ah in the first cycle at the current rate of 0.5 C/1 C (charge/discharge) and 86.4% of capacity retention after 280 cycles at 45 °C. Cells with PTEA-based GPE also showed better performance at high discharge rate (0.5 C/5 C) and 25 °C, with 92.5% capacity retention after 200 cycles. Also, in terms of safety, the most promising battery is composed of NCA/PETEA-based GPE/(graphite–Si/C). After nail penetration test of a fully charged battery, it exhibited no obvious change in contrast with NCA/LE/(graphite–Si/C), which showed a drastic swelling, followed by violent combustion when the nail penetrated into the pouch. Lastly, Ma [54] studied a cross-linked GPE based on in-situ generated poly(acrylic anhydride-2-methyl-acrylic acid-2-oxirane-ethyl ester-methyl methacrylate) (PAMM). This material is a very promising electrolyte for Li-ion batteries, because anhydride and acrylate groups can provide high voltage resistance and ionic conductivity, respectively. In agreement with this, they obtained high ionic conductivity at room temperature ($6.74 \bullet 10^{-4}$ S/cm), wide electrochemical window (5 V vs Li^+/Li), high mechanical strength (27.5 MPa), good flame resistance and excellent interface compatibility with Li metal. Then, PAMM-based GPE was further tested in $LiNi_{0.5}Mn_{1.5}O_4$/Li cells to investigate the feasibility of this material in high voltage LIBs. Thus, the first reversible capacity obtained at 0.1 C was 131.7 $mAh \bullet g^{-1}$ and after 500 cycles the discharge capacity was still 104 $mAh \bullet g^{-1}$, which corresponds to 89,5% the capacity retention with 98% of coulombic efficiency.

2.2.2. Ionic gel polymer electrolytes (IGPEs)

Most ionic gel polymer electrolytes (IGPEs) are based on ternary systems, comprised of a polymer, an ionic liquid and a lithium salt. The main advantage of these materials is related to battery safety due to the inherent physical properties of ionic liquids, such as negligible vapor pressure, non-flammability, good thermal, chemical and electrochemical stability and high ionic conductivity. Among the onium ion-based ionic liquids, imidazolium cation exhibits excellent cathodic stability and good compatibility with lithium metal anode. Hence, Karuppasamy et al. [55] synthesized 1-butyl-3-methylimidazoliumnonafluorobutane-1-sulfonate (BMImNfO), which showed a promising performance in terms of interfacial stability, cycle life and electrochemical stability when it was tested in a lithium ion battery. Thus, they prepared several IGPEs by mixing PVdF-HFP, BMImNfO and lithium nonafluoro-1-butanesulfonate (LiNfO) in different proportions, finding that the promising one was IGPE3 (80 wt. % LiNfO/ BMImNfO, 20 wt. % PVdF-HFP). This material showed high ionic conductivity (3.7 mS/cm at room temperature), lithium-ion transference number (0.44) as well as electrochemical stability window vs. Li/Li^+ (4.9 V). Then, authors tested the IGPE in a Swagelok cell containing $LiCoO_2$ as cathode material and lithium metal anode, with a cut-off voltage for charge-discharge between 3.0 and 4.2 V. The cycling performance at C/4 rate provided 138.1 mAh/g for the first cycle and upon continuous cycling, the discharge capacity decreased gradually down to 126 mAh/g on the 30th cycle, which corresponds to 91% of capacity retention.

Later, the same group [56] reported that anions with a highly electron withdrawing group possess large electrochemical windows compared to other anions. In this context, they prepared IGPEs based on PVdF-HFP, LiNfO and 1-ethyl-3-methyl-imidazolium nonafluoro-1-butanesulfonate (EMImDFOB). They presented as the most promising electrolyte the so-called ILGPE3 (80 wt. % LiNfO/IL + 20 wt. % PVdF-HFP), which has high ionic conductivity, wide electrochemical stability window and high discharge capacity at C/10 of the cathode in a $LiCoO_2$/ILGPE3/Li cell. In addition to this, the cell offered high capacity retention after 45 cycles (96% of the initial discharge capacity).

Subsequently, a similar material was reported by Karuppasamy et al. [57], after synthesizing 1-ethyl-3-methylimidazolium difluoro(oxalate) borate (EMImDFOB) ionic liquid. Ternary gel polymer electrolyte membranes were prepared by incorporating lithium difluro(oxalate) borate (LiDFOB) and EMImDFOB into a PVdF-HFP matrix. The (LiDFOB/EMImDFOB)/PVdF-HFP (80/20 wt.%) formulation (so-called DFOB-GPE3) shows an acceptable ionic conductivity ($3.3 \bullet 10^{-4}$ S/cm at 25 °C) and electrochemical stability window up to 4.46 V vs. Li/Li^+. Taking into account mechanical and thermal stabilities, high ionic conductivity and transference number, and better cyclic voltammetric performance, the DFOB-GPE3 electrolyte was tested in a $LiCoO_2$/Li coin cell at different C rates. Thus, the discharge capacity at C/10 rate is 148.4 mAh/g, and afterwards it decreases to 130 and 118 mAh/g at C/2 and 1C rates, respectively, which is from 84 to 36% of the theoretical capacity for $LiCoO_2$ active material. In parallel, at C/10 rate the cell delivers a discharge capacity of 120 mAh/g after 100 cycles, which corresponds to capacity retention of 81%, with a coulombic efficiency of 98.2% on the 100th cycle.

Recently, Balo et al. [58] investigated the effect of 1-ethyl-3-methylimidazolium bis(fluorosulfonyl)imide (EMIMFSI) on PEO-LiTFSI based GPEs. They prepared self-standing polymer membranes by solvent casting technique, obtaining films of 150–200 μm thickness. Thus, the optimized formulation of IGPE (PEO + 20 wt.% LiTFSI + 10 wt.% EMIMFSI) showed the highest value of ionic conductivity (σ) and lithium-ion transference number (t_{Li+}) at room temperature, which corresponds to a total Li-ion conductivity (σ_{Li+}) suitable for battery application (0.3 mS/cm). Moreover, the performance of this material in lithium metal batteries was studied in terms of discharge capacity, coulombic efficiency, rate capability, and capacity fading. The initial discharge capacity of cells with NCA cathode was low due to an irreversible capacity loss for SEI formation, and it takes 6 initial cycles to reach maximum discharge capacity (175 mAh/g at C/10 rate). This value remained stable throughout the cycling process and only 0.05% of total capacity was lost during 200 cycles. Furthermore, the rate capability of the Li-IGPE-NCA cell was studied, showing that at 2C rate this cell delivers 75% of NCA nominal capacity (200 mAh/g at C/10 rate). Continuing with IGPEs, Singh and co-authors [59] developed novel Li_2CuO_2-coated $LiNi_{0.33}Mn_{0.33}Co_{0.33}O_2$ (LNMC) cathode material as well as ionic liquid based gel polymer electrolytes (IL-GPE) based on a blend of PVdF-HFP, $PYR_{13}FSI$ and LiTFSI (20 wt%). The optimized IL-GPE membrane (70 wt% of $PYR_{13}FSI$) demonstrated high ionic conductivities at room temperature, σ = 3.9 mS/cm and σ_{Li+} = 1.6 mS/cm, which corresponds to a t_{Li+} = 0.43, and wide electrochemical stability window (~4.30 V vs. Li/Li^+). In parallel, the Li_2CuO_2 coating layer (20–25 nm) was uniformly formed on the surface of LNMC material with the purpose of being an electrochemical protective layer as well as enhancing the cycling performance. Thus, after 100 cycles it is observed that the specific discharge capacity of Li_2CuO_2@LNMC at 1C-rate is ~90 mAh/g with ~69% capacity retention, while the same values of pristine LNMC are ~29 mAh/g and ~30%, respectively. More recently, the same research group in a work by Srivastava et al. [60] reported ionic liquid (IL) based blend gel polymer electrolytes (BGPEs) using P(VdF-HFP) and PMMA (in the weight ratio of 3:1) as polymer matrix, 20 wt.% of LiTFSI as lithium salt and 70 wt.% of 1-ethyl-3-methylimidazolium bis(trifluoromethylsulfonyl)imide (EMIMTFSI) as IL. In addition, Ni-rich NMC cathode material was synthesized and tested with above-mentioned electrolyte in a Li cell with Li/70 wt.% IL containing BGPE/Li-rich NMC configuration. This cell delivered a maximum discharge capacity of ~166 mAh/g at 0.1 C rate within 2.4–4.2 V voltage range, retaining ~67% of the maximum capacity up to the 50th cycle.

2.3. Solid polymer electrolytes (SPE)

Solid polymer electrolytes are summarized in Table 4. Since the pioneering work by Armand et al. [61], thousands of poly(ethylene oxide) (PEO) based solid polymer electrolytes were discovered and attracted a lot of attention due to the unique combination of versatile design, good processability, high thermal stability, relatively high ionic conductivity at temperatures above 55–60 °C, good compatibility with lithium metal electrode, outstanding safety and long term durability (more than 1200

Table 4
Main features of the high voltage solid polymer electrolytes and corresponding solid-state batteries.

Solid electrolyte				WT, °C	Solid-state battery						Refs.
Formulation	δ, μm	σ,S/cm	E_{ox}, Vvs. LRE		Negative electrode	Positiveelectrode	Cycling conditions	Q_{dis1}, mAh/g	Capacityretention		
									Cycle	**%**	
P(EO/MEEGE/AGE), 82/18/2 (wt%) / LiTFSI, [O]/[Li]=16/1	50	N/A	N/A	60	Li,300 μm	$LiCoO_2$, 20 μm	3.0-4.2 V, 0.2C	120	200	63	[92]
P(EO/MEEGE/AGE) 82/18/2 (wt%) / LiTFSI, [O]/[Li]=16/1	50	N/A	N/A	50	Graphite,	$LiNi_{1/3}Mn_{1/3}Co_{1/3}O_2$,	2.5-4.2 V, 0.25C	134	5400	60	[93]
					2.5 mg/cm^2	1.3 mg/cm^2	2.5-4.2 V, 0.5C	139	1550	82	
PS-b-PPME-b-PS-$LiClO_4$, [O]/[Li]=20/1	80	$2\bullet10^{-4}$	4.5	30	Li	$LiCoO_2$	3.0-4.2 V, 0.1C	108 (4th)	100	93	[98,99]
PEO-LiTFSA	55	$1.8\bullet10^{-4}$	N/A	60	Li	$LiNi_{1/3}Mn_{1/3}Co_{1/3}O_2$	2.7-4.2 V, 0.05C	150	100	60	[94]
					Graphite		2.5-4.2 V, 0.05C	128	40	62	
PEO-PCA-LiBOB	100	$2\bullet10^{-4}$	4.6	60	Li	$LiMn_2O_4$	3.0-4.3 V, 0.5C	105	55	97.7	[100]
(10:1:2 wt%) in cellulose membrane											
P(EO/MEEGE/AGE)	55	N/A	N/A	60	Li,	$LiCoO_2$, 20 μm	3.0-4.4 V,	170	10	59	[96]
(wt 82/18/1.7)/$LiBF_4$, [O]/[Li]=16/1					300 μm	Li_3PO_4 coated $LiCoO_2$, 20 μm	0.05 mA/cm^2	174	20	76	
PEO-LiDFOB-SN	30	$8.95\bullet10^{-4}$	4.2	80	Li	$LiCoO_2$, 2.15 mg/cm^2	2.5-4.45 V, 0.1C	144.5	50	7	[75]
(10:1:9 wt.%), cellulose supported						PECA-coated $LiCoO_2$,2.15 mg/cm^2		172.8	50	60	
$P(EO)_{15}$-LiTFSI	N/A	N/A	N/A	60	Li	$LiCoO_2$	3.0-4.2 V, 0.2C	123	15	35	[97]
						LATP-coated $LiCoO_2$		128	50	93.2	
$P(EO)_8$-LiTFSI	N/A	$2\bullet10^{-5}$	N/A	50	Li	$LiMn_{0.8}Fe_{0.2}PO_4$,2.16 mg/cm^2	2.5-4.5 V, 0.1C	143	50	73	[124]
PEO-LiTFSI (71/29 wt%), [O]/[Li]=16/1	N/A	$2\bullet10^{-4}$	4.5	55	Li,200	$LiNi_{0.6}Co_{0.2}Mn_{0.2}O_2$,4.2 mg/cm^2	3.0-4.3 V, 0.1C	136.2	100	38.3	[80]
PEEC-TEGDMA-LiTFSI (17/10/73 wt%), [EC]/[Li]=1/1	<100	$1.6\bullet10^{-5}$	4.9[55]°C	25	μm			141.4	100	90.2	
PTEC-LiTFSI	30	$1.1\bullet10^{-5}$	4.5	25	Li	$LiMn_{0.8}Fe_{0.2}PO_4$,1.3-1.8 mg/cm^2	2.5-4.35 V, 0.02C	110	50	96	[102]
		$5.6\bullet10^{-5}$	N/A	55			2.5-4.35 V, 0.2C	106	100	93	
PPC-LiTFSI (10/3 wt.)	75	$3\bullet10^{-4}$	4.6	20	Li	$LiMn_{0.8}Fe_{0.2}PO_4$,5 mg/cm^2	2.5-4.35 V, 0.5C	120	100	96	[103]
in cellulose membrane											
	30	$9.8\bullet10^{-5}$	4.5	50	Li	$LiCoO_2$, 1.5 mg/cm^2	2.5-4.3 V, 0.1C	146	150	84.2	[49]
1M LiDFOB in VC [≈9.6% (w/w)]											
in cellulose separator											
PFEC-20 wt% LiDFOB in cellulose separator	N/A	$1.5\bullet10^{-4}$	5.5	25	Li	$LiNi_{0.5}Mn_{1.5}O_4$,2.9 mg/cm^2	3.0-4.9 V, 0.2C	112	50	80	[104]
					Li	$LiCoO_2$, 3.2 mg/cm^2	3.00-4.45 V, 0.1C	162	50	93	
PCL-10 wt% $LiClO_4$	2.23	$1.2\bullet10^{-6}$	5.0	25	Li	$LiNiCoO_2$, sol-gel film	2.5-4.3 V,0.01 mA/cm^2	182	50	66	[105]
PVDF–LiFSI 3/2 wt.	90	$1.18\bullet10^{-4}$	4.52	25	Li	$LiCoO_2$, 1.5 mg/cm^2	3.0-4.2 V, 0.05 mA/cm^2	141	300	71	[101]
SN-4 wt% LiBOB,	N/A	$1.4\bullet10^{-4}$	5.0	40	Li	$Li_{1.2}Mn_{0.4}Ni_{03}Co_{0.1}O_2$,5 mg/cm^2	2.5-4.6 V, 0.083C	193	20	77	[108]
separator supported											
PET/ETPTA/SN/LiTFSI (UV-cured)	25	$5.7\bullet10^{-4}$	N/A	30	$Li_4Ti_5O_{12}$	$LiCoO_2$	1.5–2.7 V, 0.2C	129	50	98	[109]
in PET nonwoven membrane							1.5–2.7 V, 1.0C	120	50	96	
P(siloxane-g-EO)LiTFSI/PEGDMA	<100	$2.5\bullet10^{-5}$	5.1	25	Li	$LiNi_{0.8}Co_{0.2}O_2$	3.0-4.1 V	130	47	99.9	[106]
O/Li: siloxane=32, PEGDMA=20											
ZI/PEO=1/20 + LiTFSI [O]/[Li]=20/1	<400	$3.39\bullet10^{-4}$	5.0	30	Li	$LiNi_{0.5}Mn_{1.5}O_4$	3.5-4.9 V, 0.1C	131.5	60	95.8	[107]
$P(EO)_{10}$-LiTFSI-$(Pyr_{14}TFSI)_2$	30	N/A	N/A	40	Li, 50 μm	$LiNi_{1/3}Mn_{1/3}Co_{1/3}O_2$,4-5 mg/cm^2	3.0-4.3 V, 0.1C	157(0.05C)	100	1	[79]
						$LiNi_{0.8}Co_{0.15}Al_{0.05}O_2$,4-5 mg/cm^2	3.0-4.3 V, 0.1C	185(0.05C)	60	60	

Note: E_{ox} – on-set oxidation potential, Q_{dis1} – first discharge capacity, WT – working temperature, CR – capacity retention

cycles) in real Li-$LiFePO_4$ solid-state batteries (SSB) [62,63]. This technology was commercialized by Bolloré group [64].

Unfortunately, SSBs with $LiFePO_4$ (LFP) cathode typically deliver specific energy lower than 200 Wh/kg due to specific properties of the cathode material, namely the average charge-discharge voltage of 3.4 V and the low specific energy. Obviously, such relatively low value is not a feasible solution for high energy batteries for the 21st century applications required to meet 500 Wh/kg energy density [65]. In turn, usage of high voltage cathode materials with high discharge capacity such as: 4 V class lithium cobalt oxide $LiCoO_2$ (LCO), various lithium nickel cobalt manganese oxides $LiNi_xMn_yCo_zO_2$ (NMC), lithium nickel cobalt aluminum oxide $LiNi_{0.8}Co_{0.15}Al_{0.05}O_2$ (NCA), lithium manganese iron phosphate $LiMn_xFe_yPO_4$ (LMFP), and 5 V class lithium nickel manganese inverse spinel $LiNi_{0.5}Mn_{1.5}O_2$ (LNMO), is widely accepted as an effective approach to increase energy density of lithium batteries [10,66–69]. In this light it is important to note that there are many published reports about extended anodic stability range up to 5 V vs. Li/Li^+ lithium reference electrode (LRE) of several advanced PEO-LiTFSI based solid polymer electrolytes, however, showing electrochemical performance in solid-state cells with LFP cathodes only [70–74]. On the other hand, it was already proved that PEO-LiTFSI based solid electrolytes are anodically stable only up to ~3.7-4.2 V vs. Li/Li^+ [69,75–78]. Therefore, without special measures, they can only be used in relatively narrow voltage range (< 4 V vs. LRE) because oxidized transition metal ions and oxygen ions in the cathode active materials will provoke the oxidative decomposition of the PEO backbone [77,79–82], especially, in the presence of $TFSI^-$ anions [82]. The possible cause of such contradictory situation is the overestimation of the oxidative stability measured by linear sweep voltammetry, due to different reasons (chemistry of semi blocking working electrode, scanning rate, slow kinetics of the decomposition reactions, formation of decomposition products with interfacial resistance, small contact area, etc.). All these factors play an important role in the real solid-state cell environment [72,78,83–86] This fact should be considered during the development of high voltage solid-state batteries.

Several recent reviews with comprehensive analysis of different types of solid electrolytes have been published [72–73,87–89,90,91]

Non-exhaustive lists of solid polymer and hybrid electrolytes analyzed in this work are presented in Table 4 and Table 5, respectively.

It is interesting to note that despite limited electrochemical stability, polyethylene oxide and its derivatives (among the ancient materials in this field) have always been and seem to remain one of the most popular classes of polymeric materials used for the development of solid polymer electrolytes. Below we describe several interesting strategies to adapt PEO based SPEs in high voltage batteries reported by various groups.

In 2001, Matsui et al. [92] synthesized P(EO/MEEGE/AGE) polymer by ring opening copolymerization of ethylene oxide (EO), 2-(2-methoxyethoxy)ethyl glycidyl ether (MEEGE), and allyl glycidyl ether (AGE), and by its mixing with lithium bis(trifluoromethanesulfonyl)imide (LiTFSI) prepared solid polymer electrolyte. The solid-state cell $LiCoO_2$/P(EO/MEEGE/AGE) + LiTFSI/Li cycled at 60 °C delivered 160 mAh/g on the first cycle and gradually decreased by 0.13% per cycle for 200 cycles. Later, Kobayashi et al. [93] developed a high voltage solid-state lithium-ion battery based on NMC111 cathode, natural graphite anode and P(EO/MEEGE/AGE)-LiTFSI solid polymer electrolyte. The SSB demonstrated outstanding and best ever reported capacity retention, maintaining 80% of initial capacity after 1550 cycles at 60 °C. The decrease of operating temperature to 50 °C significantly improves the battery cycle life which can retain 60% of initial capacity after 5400 cycles. This fact strongly supports the hypothesis that polyether-based SPEs can be used in cells with 4.2 V charge cut-off voltage region with cathode/SPE interface stabilizing an electrochemically stable catholyte comprised by lithium bis(oxalate)borate (LiBOB) and Tetrakis [methylene-3(30,50 edi-tert-butyl-40-hydroxyphenyl) propionate] methane (Antioxidant 1010) [93].

Another solvent-free solid polymer electrolyte based on PEO-LiTFSA (lithium bis(trifluoromethanesulfonyl)amide) mixture was prepared and tested by Seki [94], in 4 V-class solid-state lithium and lithium-ion polymer batteries with NMC111 cathodes. The performance of the lithium metal SSB reached 100 cycles with 60% of initial capacity due to stabilization of cathode/SPE interface by mixing $LiAlO_2$ powder with the positive electrode materials. In turn, lithium-ion solid polymer cell with the same cathode and SPE demonstrated worse performance: 40 cycles until reaching 62% of initial capacity.

Surface protection (or coating) of high voltage cathode materials by inorganic substances (ferroelectric $LiNbO_3$, lithium ion conductor $LiAlO_2$, metal oxides and phosphates etc.) is a well-known method to improve their compatibility with liquid and sulfide inorganic electrolytes and, in this way, reduce resistance of cathode/solid electrolyte interface [10,95]. In this light, Seki and co-authors [96] reported improved electrochemical behavior of Li/P(EO/MEEGE/AGE)-$LiBF_4$/$LiCoO_2$ solid-state cell with Li_3PO_4-coated $LiCoO_2$ particles (4.1 vs. 1.2 %/cycle). However, the coating has quite limited effect because the cathode/SPE interface degradation could be only partially controlled via active material coating due to intrinsic instability of the used P(EO/MEEGE/AGE)-$LiBF_4$ solid polymer electrolyte. Later, Ma et al. [75] suggested to introduce a poly(ethyl α-cyanoacrylate) (PECA) buffer layer in between solid polymer electrolyte and $LiCoO_2$ cathode. As a result, Li/PEO-LiDFOB-SN/PECA-$LiCoO_2$ cell demonstrated better electrochemical performance: initial discharge capacity and capacity retention (1.9 vs. 0.8 %/cycle) in comparison with reference cell with positive electrode based on uncoated lithium cobalt oxide. Authors revealed that PECA coating has multiple effects: decreasing the oxidation ability of $LiCoO_2$, suppression of the decomposition of LiDFOB, and maintaining the interaction between PEO and LiDFOB during high voltage cycling. Nevertheless, the achieved progress on cyclability of the investigated solid-state cell is still far from threshold allowing its practical use. In 2018, Yang et al. [97] synthesized $Li_{1.4}Al_{0.4}Ti_{1.6}(PO_4)_3$ (LATP) coated $LiCoO_2$ showing improved capacity retention (4.3 vs. 0.13 %/cycle) in a solid-state cell with $P(EO)_{15}$-LiTFSI SPE due to restrained side reaction between PEO and $LiCoO_2$. However, even cells with stabilized surface protected LCO cathode demonstrated low coulombic efficiency, especially on first cycles.

A trend on partial replacement of PEO and its derivatives is evident. For example, Niitani et al. [98–99] reported triblock copolymer based PS-b-PPME-b-PS-$LiClO_4$ (PPME-poly(ethylene glycol) methyl ether methacrylate, PS-polystyrene) solid polymer electrolyte with microphase separation and, as result, high ionic conductivity at 30 °C, improved mechanical stability, and wide electrochemical stability range up to 4.5 V. High voltage solid-state Li/SPE/$LiCoO_2$ battery showed good capacity retention (93% after 100 cycles) at 30 °C. Partial replacement of PEO by poly (cyano acrylate) (PCA) was discovered by Zhang [100]. Rigid-flexible solid polymer electrolyte prepared by dispersion of PEO-PCA-LiBOB mixture in cellulose nonwoven membrane (CNM) demonstrated extended electrochemical stability range (4.6 V vs. LRE) due to the synergetic effect between PCA and nonwoven cellulose. As a result, solid-state cell Li/PEO-PCA-LiBOB-CNW/$LiMn_2O_4$ demonstrated very stable capacity retention (97.7% after 55 cycles at 60 °C) indicating that the solid polymer electrolyte is compatible with high voltage cathode materials.

Ionic liquids are widely used class of materials in high voltage lithium batteries with liquid electrolytes due to their exceptional thermal stability and electrochemical stability range. For instance, PEO-LiTFSI-PYR_{14}TFSI (N-butyl-N-methylpyrrolidinium bis(trifluoromethanesulfonyl) imide) based solid polymer electrolyte (Fig. 5, Area 2) with $LiNi_{1/3}Mn_{1/3}Co_{1/3}O_2$ and $LiNi_{0.8}Co_{0.15}Al_{0.05}O_2$ 4 V-class cathodes in solid-state batteries was investigated by Wetjen et al. [79]. It has been discovered that $LiNi_{1/3}Mn_{1/3}Co_{1/3}O_2$ based cell degraded much faster in comparison to $LiNi_{0.8}Co_{0.15}Al_{0.05}O_2$ one due to different degradation mechanisms. In particular, capacity fade (100 cycles until reaching 60% of initial capacity) of NCA based cell is attributed

Table 5
Main features of the high voltage hybrid electrolytes and corresponding solid-state batteries.

Solid electrolyte				WT, °C	Solid-state battery						Refs.
Formulation	δ, μm	σ,S/cm	E_{ox}, Vvs. LRE		Negative electrode	Positiveelectrode	Cycling conditions	Q_{dis1}, mAh/g	Capacityretention Cycle	%	
PEO_{19}-$Li(CF_3SO_2)_2N$-10 wt% $BaTiO_3$	N/A	N/A	N/A	80	Li	$LiNi_{0.8}Co_{0.2}O_2$, 200 μm	2.5-3.8 V,0.2 mA/cm^2	100	25	94	[77]
							2.5-3.9 V,0.2 mA/cm^2	130	35	83	
							2.5-4.0 V,0.2 mA/cm^2	136	27	64	
PEO_{10}-($LiN(CF_3SO_2)_2$/ 10 wt% $BaTiO_3$, [O]/[Li]=10/1	300	$1.2\bullet10^{-3}$	4.2	80	Li	$LiNi_{0.8}Co_{0.2}O_2$, 40 μm	2.5-4.2 V,0.2 mA/cm^2	154	40	79	[78]
(PEO_{10}-($LiN(CF_3SO_2)_2$-10 wt% $LiPF_6$)/ 10 wt% $BaTiO_3$, [O]/[Li]=10/1	300	$6.7\bullet10^{-4}$	5.0	80	Li			150	89	75	
PEO-10 wt.% HBP $Li(CF_3SO_2)_2N$- 10 wt.% $LiPF_6$/10 wt% $BaTiO_3$, [O]/[Li]=10/1	200	$1.5\bullet10^{-3}$	>4.0	60	Li	$LiNi_{0.8}Co_{0.2}O_2$, 40 μm	2.5-4.2 V,0.2 mA/cm^2	108	30	99.9	[114]
							2.5-4.4 V, 0.57C,0.2 mA/cm^2	154	410	48	
$P(EO)_8/LiClO_4$ + 20 wt% $Li_{6.28}Al_{0.24}La_3Zr_2O_{12}$	<150	$4.4\bullet10^{-4}$	4.5	30	Li	$LiCoO_2$,5 mg/cm^2	3.0-4.2 V, 0.06C, 0.05 mA/cm^2	142	30	85	[86]
PEO_{20}/LiTFSI + 5 wt% $Li_{6.28}Al_{0.24}La_3Zr_2O_{12}$	100	$7.7\bullet10^{-4}$(30°C)	4.5	25	Li	$LiNi_{1/3}Mn_{1/3}Co_{1/3}O_2$	2.6-4.3 V, 0.1C	158	100	76	[120]
PEO-LiTFSI + 20 wt% $Li_{3/8}Sr_{7/16}Ta_{3/4}Zr_{1/4}O_3$	N/A	$3.5\bullet10^{-4}$	5.2	45	LI	$LiNi_{0.8}Mn_{0.1}Co_{0.1}O_2$	2.8-4.3 V, 50 μA/cm^2	146	120	81.5	[121]
$P(EO)_{18}$-LiTFSI-1 wt% $Li_{10}GeP_2S_{12}$	N/A	$5\bullet10^{-4}$	5.7[80]°C	60	Li	$LiCoO_2$	3.0-4.25 V, 0.1C	125	N/A	N/A	[117]
PEO + wheat flour (9/1 wt.)	N/A	$2.62\bullet10^{-5}$	5.5	25	Li, 300 μm	$LiNi_{0.8}Co_{0.1}Mn_{0.1}O_2$	2.5-4.2 V, 0.1C	133	60	47	[115]
+ 40 wt% LiTFSI		$2.5\bullet10^{-3}$	5.1	100			2.5-4.2 V, 1C	158	5	84	
HBPS-PB-PPEGMA/LiTFSI + alumina nanowire film	N/A	$2.5\bullet10^{-4}$	5.2	50	Li	$LiCoO_2$,4-5 mg/cm^2	3.0-4.3 V, 0.1C	135	40	72	[116]
$P(EO)_{15}$-$LiClO_4$, 52.5 wt% $Li_7La_3Zr_2O_{12}$	100	$4.4\bullet10^{-4}$	5	55	Li	$LiNi_{0.6}Mn_{0.2}Co_{0.2}O_2$, 2 mg/cm^2	2.5-4.3 V, 0.02C	166	N/A	N/A	[118]
PEO-$Li_{6.4}La_3Zr_{1.4}Ta_{0.6}O_{12}$ (12 wt%)	40	$5.4\bullet10^{-4}$	4.75	60	Li, 50 μm	$LiFe_{0.15}Mn_{0.85}PO_4$,1.4 mAh/cm^2	2.5-4.3 V, 0.1C	120	200	83	[119]
PEO-$Li_{1.5}Al_{0.5}Ge_{1.5}(PO_4)_3$ (1/99 wt%)	N/A	$0.5\bullet10^{-4}$	5.12	50	Li	$LiMn_{0.8}Fe_{0.2}PO_4$,2.16 mg/cm^2	2.5-4.5 V, 0.1C	165	50	94	[124]
Li_6PS_5Cl + 5 wt% PEO	N/A	$1.6\bullet10^{-4}$	N/A	30	Li	$LiNi_{0.8}Mn_{0.1}Co_{0.1}O_2$	2.5.-4.0 V, 0.05C	100	200	91	[122]
		$7.8\bullet10^{-4}$		60			2.5.-4.0 V, 0. 5C	60	500	44	
PEO_{10}LiTFSI+ 5 wt% $LiNO_3$ + 5 wt% LiBOB + 10 wt. % of halloysite nanoclay	N/A	$3\bullet10^{-4}$	4.6	60	LI	$LiNi_{1/3}Mn_{1/3}Co_{1/3}O_2$, 3-4 mg/cm^2	3.0-4.2 V. 0.2C	100	55	120	[123]
P(PC)-LiTFSI (4/1 wt)/ $Li_{6.75}La_3Zr_{1.75}Ta_{0.25}O_{12}$ (5 wt%)	N/A	$5.2\bullet10^{-4}$	4.6	25	Li	$LiFe_{0.2}Mn_{0.8}PO_4$,32 μm	2.5-4.4 V, 0.5C	110	80	83	[125]
$P(BA)_6$-$LiClO_4$-$Li_{1.5}Al_{0.5}Ge_{1.5}(PO_4)_3$ (80 wt%)	N/A	$3\bullet10^{-5}$	4.7	55	Li, 200 μm	$LiNi_{0.6}Mn_{0.2}Co_{0.2}O_2$,6 mg/cm^2	3.0-4.2 V, 0.2C	163	100	80	[126]
PVdF-10 wt% ($Li_{6.75}La_3Zr_{1.75}Ta_{0.25}O_{12}$-$LiClO_4$)	N/A	$5.4\bullet10^{-4}$	N/A	25	Li	$LiCoO_2$	3.0-4.2 V, 0.4C	150	120	98	[127]
7.5 wt% LLZO-PPC-LiTFSI supported by a cellulose fabric (covered by pensil)	70	$1.59\bullet10^{-4}$	4.6	25	Li	$LiNi_{0.6}Mn_{0.2}Co_{0.2}O_2$,2.9-3.0 mg/cm^2	2.7-4.3V, 0.3C	162	200	65	[128]
LLZO-Py_{14}TFSI-LiTFSI (80/19/1 wt%)	150	$0.4\bullet10^{-3}$	5.5	25	Li	$LiCoO_2$, 3 mg/cm^2	3.0-4.3 V, 0.1C	144	150	76	[129]
0.2M LiTFSI, 0.8M PYR_{14}TFSI,	150	$1.3\bullet10^{-3}$	5.025°C	30	Li	$LiCoO_2$,60 μm, 4.7 mg/cm^2	3.0-4.2 V, 0.1C	118	50	99	[130]
60 wt% $BaTiO_3$		$8\bullet10^{-3}$		80				135	70	87	

to high charge cut-off voltage, most likely due to formation and growth of a surface film at the cathode/polymer electrolyte interface. On the other hand, authors did not prove continuous decomposition of the SPE whereas showing that the presence of $PYR_{14}TFSI$ ionic liquid significantly decreased interfacial resistance and diminished the dissolution of aluminum corrosion products into the electrolyte.

Beyond PEO based polymers, several such alternative polymer hosts (polycarbonates, polysiloxanes, polyesters, PVdF, etc.) suitable for using in solid polymer electrolytes compatible with high voltage cathodes have been already discovered [74,101].

Recently, Jung et al. [80] synthesized cross-linked solid polymer electrolyte based on amorphous poly(ethylene ether carbonate) (PEEC), tetraethyleneglycol diacrylate (TEGDA) and LiTFSI salt with improved ionic conductivity, electrochemical stability and lithium transference number compared with PEO. PEEC backbone and high salt concentration ([EC]/[Li] as 1/1) of the developed SPE extended its electrochemical stability range (4.9 V) comparing with PEO-based one (4.5 V). Subsequently, the developed SPE exhibited very good capacity retention (90.2% after 100 cycles) in $Li/LiNi_{0.6}Co_{0.2}Mn_{0.2}O_2$ solid-state cell cycled at 25 °C. He and co-authors [102] reported carbonate-linked PEO solid polymer poly(triethylene glycol carbonate) (PTEC) as a base of solid polymer electrolyte PTEC-LiTFSI which demonstrated very stable electrochemical performance in $Li/LiFe_{0.2}Mn_{0.8}PO_4$ cells at 25 °C and 55 °C due to extended electrochemical stability window (4.5 V). Safety-reinforced poly(propylene carbonate) (PPC)-LiTFSI solid electrolyte proposed by Zhang [103] displayed very high ionic conductivity at 20 °C and extended range of anodic stability (4.6 V). Consequently, high voltage $Li/LiFe_{0.2}Mn_{0.8}PO_4$ solid-state cell cycled at 60 °C showed impressive stability of charge-discharge profiles and capacity retention (96% after 100 cycles). In addition, Chai et al. [49] proposed a novel in-situ generated poly (vinylene carbonate) (PVC)-LiDFOB solid polymer electrolyte with superior electrochemical stability window (4.5 V) and considerable ionic conductivity ($9.8\bullet10^{-5}$ S/cm at 50 °C). High voltage solid-state cell with lithium anode and $LiCoO_2$ cathode showed high-capacity retention (84.2% after 150 cycles) indicative of good interfacial stability and excellent cycling performance during long-term cycles.

Novel poly(vinylidene difluoride) (PVdF)-LiFSI based solid electrolyte proposed by Zhang at al. [101] showed high ionic conductivity ($1.18\bullet10^{-4}$ S/cm at 25 °C) and good compatibility with lithium anode. In addition, 200 cycles of $Li/LiCoO_2$ at 25 °C were demonstrated. It is important to note that the lithium salt choice is important for high voltage stability of solid electrolytes. The best performance was obtained with LiFSI salt whereas solid electrolytes based on LiTFSI and $LiClO_4$ salts demonstrated very poor electrochemical performance.

High-voltage-tolerated polymer electrolyte (HVTPE) based on poly(fluoroethylene carbonate) (PFEC), synthesized through ring-opening polymerization, and 20 wt% of LiDFOB incorporated into cellulose separator has been discovered by Liu et al. [104], The developed HVTPE demonstrated good ionic conductivity of $1.5\bullet10^{-4}$ S/cm and high anti-electro-oxidation ability (up to 5.5 V) at 25 °C. Such remarkable electrochemical properties enable excellent cyclability of 4V $Li/LiCoO_2$ and 5 V solid-state $Li/LiNi_{0.5}Mn_{1.5}O_4$ cells at room temperature.

Fonseca et al. [105], prepared thin solid polymer electrolyte films based on polycaprolactone (PCL) and 10 wt. % of $LiClO_4$ salt. The SPE showed relatively low ionic conductivity $1.2\bullet10^{-6}$ S/cm at 25 °C but extended range of the electrochemical stability (5 V). Solid-state $Li/LiNiCoO_2$ cell based on the developed SPE delivered 182 mAh/g on the first discharge and 120 mAh/g after 50 cycles.

Oh et al. [106], prepared cross-linked mono-comb type poly(siloxane-g-ethyleneoxide)-LiTFSI based solid polymer electrolyte with high ionic conductivity at near room temperature, high thermal stability and high oxidation potential (5.1 V) due to the presence of siloxane bond as a backbone of the main component, LiTFSI–PEO complexation and cross-linked structure. Therefore, $Li/SPE/LiNi_{0.8}Co_{0.2}O_2$ solid-state cell delivered 130 mAh/g on first charge and outstanding capacity retention of 99.9% after 47 cycles at 25 °C. Recently, Liu et al. [107], synthesized a novel solid-state polymer electrolyte based on zwitterion (ZI) and poly(ethylene oxide) substituted polysiloxane mixed with LiTFSI salt. The ZI addition improved the electrochemical properties (ionic conductivity, electrochemical window, interfacial stability, and lithium-ion transference number) of the SPE. As result, 5 V-class solid-state $Li/LiNi_{0.5}Mn_{1.5}O_4$ cell demonstrated excellent cycle performance (95.8% after 50 cycles).

Plastic crystal electrolytes based on nitrile materials are widely investigated as candidate materials for high voltage solid-state batteries due to their high thermal stability, high ionic conductivity, and wide electrochemical stability window. However, pure nitrile based electrolytes cannot be used in a self-standing form and require mechanical reinforcement [72]. For example, Abouimrane and Davidson [108] investigated solid electrolyte based on succinonitrile (SN) doped with 4 wt. % of LiBOB salt. This SPE demonstrated good compatibility with lithium metal, good ionic conductivity ($1.4\bullet10^{-4}$ S/cm at 40 °C) and wide electrochemical stability range (5 V vs. LRE at 40 °C), good enough for practical use in SSB. However, capacity fade of Li/SN–4% $LiBOB/Li_{1.2}Mn_{0.4}Ni_{0.3}Co_{0.1}O_2$ solid-state coin cell was quite high (1.15 %/cycle) in contrast to Li/SN–4% $LiBOB/LiFePO_4$ cell. In 2013, Choi et al. [109], fabricated very thin, deformable and safety reinforced (with PET) nonwoven membrane plastic crystal polymer electrolyte based on UV-cured ETPTA cross-linker and SN-LiTFSI system. The proposed solid electrolyte demonstrated improved mechanical properties, high ionic conductivity at 30 °C, and very stable electrochemical performance (0.08 %/cycle) in $Li_4Ti_5O_{12}/LiCoO_2$ solid-state cell working under 1C charge-discharge current.

It is interesting to note that despite the fact of limited electrochemical stability, polyethylene oxide and its derivatives have always been and seem to remain one of the most popular class of polymer materials used for the development of solid polymer electrolytes.

2.4. Hybrid electrolytes (HE)

Hybrid electrolytes are summarized in Table 5. Hybridization is a well-known and effective method to exploit advantages and overcome disadvantages of each component of complex mixtures [110–112]. In this context, hybrid polymer/inorganic electrolytes can be considered as an ultimate solution to benefit of the advantages of each component: the processability, flexibility, wettability of polymers and chemical, thermal and electrochemical stability, ionic conductivity and mechanical properties of inorganic materials [69,113].

PEO based solid polymer electrolytes suffer of poor mechanical stability at common SSB battery operating temperature (> 50 °C). The use of inorganic fillers to improve mechanical stability of PEO-based SPEs can be considered as a very efficient strategy among others. Generally speaking, the inorganic part of hybrid electrolytes can be represented by two types of fillers: inert and lithium conductive ones.

A multitude of inactive fillers were reported for low voltage systems (e.g. Li-S, $Li-LiFePO_4$). However, to the best of our knowledge only two fillers ($BaTiO_3$ and wheat flour) were used in PEO-based electrolytes developed for high voltage SSBs. In 2001, Li et al. [77] showed that the addition of 10 wt. % of $BaTiO_3$ powder in PEO_{19}-$Li(CF_3SO_2)_2$ solid polymer electrolyte improves the interfacial stability and, as a result, the electrochemical performance of solid-state $Li/LiNi_{0.8}Co_{0.2}O_2$ cell operating in 2.5–3.9 V cycling range at 80 °C. The same SSB cycled in narrower 2.5–3.8 V cycling range showed better capacity retention but on 30% lower discharge capacity, whereas increasing charge cut off voltage up to 4.0 V does not increase initial capacity but drastically decrease cyclability due to electrochemical decomposition of the solid electrolyte. Through these authors demonstrated that charge cut off voltage is a crucial factor for SSBs to find an optimal trade-off between specific energy density and cycle life. Later, the same group reported a hybrid solid electrolyte (PEO_{10}–($LiN(CF_3SO_2)_2$-10 wt. % $LiPF_6$) and 10 wt. % of $BaTiO_3$ with improved electrochemical stability range and

enhanced electrochemical performance in $Li/LiNi_{0.8}Co_{0.2}O_2$ solid-state battery, attributed to the suppression of aluminum current collector corrosion by adding 10 wt. % of $LiPF_6$ salt [78]. In 2003, the same authors [114] developed enhanced hybrid solid electrolyte based on PEO, hyperbranched polymer poly[bis(triethylene glycol) benzoate] with terminal acetyl groups (HBP), $Li(CF_3SO_2)_2N$ (LiTFSI), $LiPF_6$, and $BaTiO_3$ with high ionic conductivity of 10^{-4} S/cm at room temperature. Moreover, high voltage $Li/LiNi_{0.8}Co_{0.2}O_2$ solid-state cell tested in 2.5–4.4 V cycling range at 60 ˚C demonstrated quite stable capacity retention (48% after 410 cycles) attributed to positive impact of HBP, $BaTiO_3$ and, especially, $LiPF_6$ salt. Lin et al. [115] synthesized biodegradable solid composite electrolyte based on PEO-LiTFSI system with addition of 10 wt. % of wheat flour which is compatible with the polymer matrix due to existing –C–O–, –N–, and –C=O functional groups that can coordinate with lithium ions like –C–O–C– in PEO to form Li^+ ion diffusion channels and reduce crystallinity of the polymer matrix. Despite improvement of electrochemical stability range, high voltage solid-state Li/PEO-LiTFSI-Flour/$LiNi_{0.8}Co_{0.1}Mn_{0.1}O_2$ (NMC811) battery showed relatively poor electrochemical performance at 25 ˚C and, especially, 100 ˚C caused by instability of the cathode/HE interface.

Wang et al have proposed to prepare a composite electrolyte by casting the SPE solution (polymer/THF/LiTFSI) onto free-standing aluminum oxide electrostatic spinning film containing ceramic nanowires [116]. The prepared solid electrolyte showed a high ionic conductivity of $9.63•10^{-5}$ S/cm and, most importantly, the introduction of poly(pinacol vinylboronate) segments onto the hyperbranched polymer strongly improves the electrochemical stability up to 5.2 V at 50 ˚C. Nevertheless, $Li/LiCoO_2$ cell cycled at 50 ˚C and 0.1 C demonstrated relatively stable electrochemical performance maintaining just 72% of initial discharge capacity after 40 cycles.

In turn, several hybrid electrolytes with Li-ion conductive fillers were reported. Zhao et al. [117] demonstrated good charge-discharge cycle performance of $Li/LiCoO_2$ solid-state battery with solid composite polymer electrolyte PEO-LiTFSI with addition of 1 wt. % of $Li_{10}GeP_2S_{12}$ lithium ion conductive filler. However, no more cycles have been performed in contrast with $Li/LiFePO_4$ cell with the same solid electrolyte. In turn, Choi et al. [118] investigated hybrid solid electrolyte based on PEO-$LiClO_4$ system with addition of 52.5 wt. % of $Li_7La_3Zr_2O_{12}$ lithium ion conductive filler. On the first, solid-state Li/NMC622 cell showed relevant charge-discharge capacity and high initial coulombic efficiency (87.8%) that is superior compared to the cells with alumina doped and undoped PEO-$LiClO_4$ solid electrolytes. Zhang et al. [119] studied Li-salt free solid composite electrolyte based on PEO and 12 wt. % nanometric filler with garnet structure $Li_{6.4}La_3Zr_{1.4}Ta0_{.6}O_{12}$. High voltage solid-state $LiFe_{0.15}Mn_{0.85}PO_4$/PEO-$Li_{6.4}La_3Zr_{1.4}Ta_{0.6}O_{12}$/Li cell demonstrated good C-rate capability and cycle performance due to addition of LLZTO nanofillers which improves the oxidation stability of the whole HE. Nevertheless, authors suggested using polymer with improved electrochemical stability to satisfy requirements for high energy density and safe solid-state batteries. Recently, Karthik and Murugan [86] published a research regarding PEO-$LiClO_4$-$Li_{6.28}Al_{0.24}La_3Zr_2O_{12}$ solid electrolyte possessing maximum ionic conductivity when filler content is 20 wt. % (0.44 mS/cm at 30 ˚C). Despite extended electrochemical stability range (4.5 V), solid-state $Li/LiCoO_2$ cell demonstrated fast capacity decay and relatively low coulombic efficiency (96% on the 30th cycle) probably caused by loss of active material, lithium inventory, and formation of a SEI in the lithium anode increasing cell impedance. Later, the same authors have published experimental results [120] of hybrid electrolytes with 5 wt.% of $Li_{6.28}Al_{0.24}La_3Zr_2O_{12}$ (LLZA) garnet filler (particles size ~150 nm) incorporated into PEO_{20}/LiTFSI dry solid polymer electrolyte membrane (DSPEM-5) with high lithium conductivity of $7.7•10^{-4}$ S/cm at 30 ˚C. The coin cell $LiNi_{0.33}Mn_{0.33}Co_{0.33}O_2$/Li with integrated DSPEM-5 hybrid electrolyte membrane demonstrated an impressive electrochemical performance delivering 158 mAh/g at 0.1 C with 98% of coulombic efficiency and showing 76% of capacity retention after 100 cycles at 25 ˚C.

Xu et al. [121] reported a flexible and low-cost PEO/LiTFSI/perovskite $Li_{3/8}Sr_{7/16}Ta_{3/4}Zr_{1/4}O_3$ composite electrolyte with a Li-ion conductivity of $3.5•10^{-4}$ S/cm at 45 ˚C. Addition of the perovskite extends the electrochemical window up to 5.2 V at 45 ˚C. Consequently, the Li/NMC811 solid-state cell with this composite electrolyte demonstrated reasonable cycling performance with initial discharge capacity of 146 mAh/g and 81.5% capacity retention after 120 cycles at 45 ˚C.

Zhang et al. [122] proposed the addition of 5 to 20 wt.% poly(ethylene oxide) to argyrodite Li_6PS_5Cl to enhanced mechanical properties and form a stable lithium/electrolyte interface. As results, solid-state battery Li/NMC811 equipped with inorganic rich hybrid electrolyte with 5 wt.% of PEO at 0.05C, 2.5–4.0 V and 30 ˚C could maintain of 91% of initial relatively low discharge capacity of 100 mAh/g over 200 cycles showing high coulombic efficiency excepting the 1st cycle. At the same time, increasing operation temperature to 60 ˚C provokes twice-faster capacity decay (54%) after 500 cycles.

In turn, Zhao and coauthors [123] have demonstrated a simple strategy significant improving the electrochemical stability of composite PEO-halloysite nanoclay electrolytes via tri-salt cocktail: $LiNO_3$ as a SEI former; LiTFSI as an easily dissociated charge carrier for bulk ion transport; and LiBOB as an effective CEI former. As result, Li/NMC111 solid-state cell showed a specific capacity over 100 mAh/g after 60 cycles with coulombic efficiency of 99 % during cycling at 60 ˚C and 3.0–4.2 V voltage interval.

Since PEO has quite limited electrochemical stability, Wang et al. [124] suggested drastically reducing its content in formulations in order to improve the electrochemical stability of the final solid electrolyte. Consequently, “polymer-in-ceramic” type composite electrolyte containing just 1 wt. % of PEO and 99 wt. % of $Li_{1.5}Al_{0.5}Ge_{1.5}(PO_4)_3$ (LAGP) ceramic powder tested in $Li/LiMn_{0.8}Fe_{0.2}PO_4$ solid-state battery at 50 ˚C showed higher initial discharge capacity and capacity retention in comparison with reference cell based on PEO-LiTFSI solid polymer electrolyte.

PEO replacement, by more electrochemically stable polymer matrix, is an effective way to improve compatibility of solid electrolytes with high voltage cathode materials. As additional illustration of this thesis, free-standing poly(propylene carbonate(PPC)-$Li_{6.75}La_3Zr_{1.75}Ta_{0.25}O_{12}$ (LLZTO)-LiTFSI composite solid electrolyte was proposed by Zhang [125] Solid-state $Li/LiFe_{0.2}Mn_{0.8}PO_4$ battery demonstrated promising cycle life (83.1% of initial capacity after 80 cycles) at room temperature due to high ionic conductivity, wide electrochemical stability window and superior compatibility of the PPCL-LZTO-LiTFSI hybrid electrolyte with high voltage LMFP electrode. In turn, Park and co-authors [126] reported hybrid electrolyte based on poly(1,4-butylene adipate) (PBA) polymer mixed with $LiClO_4$ and 60–80 wt. % of $Li_{1.5}Al_{0.5}Ge_{1.5}(PO_4)_3$ lithium ion conductive ceramic particles. The $Li/LiNi_{0.6}Co_{0.2}Mn_{0.2}O_2$ all-solid-state cell with hybrid electrolyte containing 80 wt. % of LAGP demonstrated high discharge capacity on the first cycle (163 mAh/g) and good capacity retention (80% after 100 cycles) at 55 ˚C due to high ionic conductivity and improved electrochemical stability of PBA polymer (4.7 V vs. LRE). Zhang et al. prepared a solid hybrid electrolyte based on $Li_{6.75}La_3Zr_{1.75}Ta_{0.25}O_{12}$ (LLZTO) ceramics, poly(vinylidene fluoride) (PVDF) and $LiClO_4$ salt [127]. The structurally modified electrolyte demonstrated enhanced electrochemical performance at 25˚C, satisfactory mechanical properties, and good thermal stability due to partial PVdF dehydrofluorination enhancing the interactions between the PVDF matrix, lithium salt, and LLZTO particles. In particular, $Li/LiCoO_2$ solid-state cell demonstrated high initial discharge capacity (150 Ah/g) and capacity retention (98% after 120 cycles). In turn, Jing and co-authors [128] proposed LLZO (0.2Al-$Li_7La_3Zr_2O_{12}$) fibers-filled PPC/LiTFSI composite solid electrolyte partially supported by a cellulose fabric. This system showed high potential window exceeding 4.6 V and a high ionic conductivity of $1.59•10^{-4}$ S/cm at ambient temperature. Li/NMC622 solid-state cell equipped with 7.5 wt.% LLZO-PPC-LiTFSI composite electrolytes having interfacial modification demon-

strated promising electrochemical performance due to the synergetic effect of LLZO fibers and graphite coating.

An interesting concept of hybrid pseudo solid electrolyte (Fig. 5, Area 4) with immobilized ionic liquid composed by a blend of $Li_7La_3Zr_2O_{12}$ (LLZO) powder, 1-butyl-1-methylpyrrolidinium bis (trifluoromethylsulfonyl) imide ($PYR_{14}TFSI$) ionic liquid, and LiTFSI salt was proposed by Kim and co-authors [129]. The $Li/LiCoO_2$ pseudo solid-state cell equipped with the LLZO-$PYR_{14}TFSI$-LiTFSI hybrid electrolyte showed relevant discharge capacity and good capacity retention after 150 cycles at 25 °C. This result clearly demonstrated that eliminating a polymer from the solid electrolyte is an effective way to improve real high voltage stability. Later, a nanocomposite quasi-solid-state electrolyte LiTFSI-$Pyr_{14}TFSI$-$BaTiO_3$ with high thermal stability, a wide electrochemical window, good ionic conductivity at 30°C, and a remarkably high lithium-ion transference number was reported by Choi et al. [130] Subsequently, $Li/LiCoO_2$ solid-state cells prepared using this nanocomposite solid electrolyte exhibited high electrochemical performance at 25 °C and 80 °C. However, processability and flexibility of such hybrid electrolytes could be far from ideal.

2.5. Solid inorganic electrolytes

Solid inorganic electrolytes are among the most widespread solid electrolyte families, because of their peculiarities [131–135].

Ceramic glass ion conductors are being developed to replace the current liquid electrolyte and even separator as well since robust solid electrolyte can isolate the cathode from anode and resist the growth of Li dendrites as well, and therefore enhances the safety of lithium-ion batteries [136].

Since the basic configuration and crystalline structure, and the comparison of Li ionic conductivity of all the solid electrolytes have been well described by Bachman [137] only the recent progress of inorganic electrolytes with the typical four structures (thus Garnet, LISICON, NASICON, and Perovskite) is reviewed in this paper and in a sequence according to the involved research activities reported contemporarily.

2.5.1. Garnet structured electrolytes

Due to the high Li ionic conductivity of garnet structured electrolyte $Li_7La_3Zr_2O_{12}$ (LLZO), a great deal of research has been carried out on improving the Li ion diffusion of LLZO and the development of all-solid-state lithium-ion batteries based on LLZO electrolyte.

There are two kinds of structures of garnet structured LLZO, thus tetragonal and cubic structured LLZO phases, where the Li ionic conductivity of the tetragonal phase much higher than that of the cubic phase [138]. A series of improvement on the stabilization of the cubic phase [138]. LLZO again tetragonal phase have been performed via doping (Al, Ga, Fe, Mo, etc.) [139–141]. A high Li ionic conductivity of ~1.46 mS/cm has been achieved in Ga doped LLZO (containing 0,25 Ga atoms per formula unit)[142].

In order to understand the occupation of doping atoms in the LLZO lattice and the corresponding influence on the Li ionic conductivity, some theoretical work has been performed to investigate the possible Li pathway in the lattices of undoped and doped LLZO. According to the bond valence method (BVM), in the multiple doped LLZO with Al and Ta element, Al atom tends to occupy the 96 h position in the case of co-doping of LLZO by Al and Ta instead of the 24d position when only Al is used for doping, which helps to reduce the impeding effect of Al at 24d position to the Li diffusion in the lattice of LLZO while still keeps the cubic structure, as shown in Fig. 7 [143].

Besides the theoretical investigation of Li ionic diffusion in the lattice of LLZO, some practical improvement has been achieved in the Li ionic conductivity in LLZO. Isabel N. David et al adopted the hot-isostatic-pressing (HIP) sintering processes to prepare highly densified cubic LLZO materials to reduce the contribution of grain boundary to the total Li ionic conductivity to about 8% [144]. Li_3BO_3 have been added as sintering aid to enhance the high temperature sintering process to form densified ceramic pellet [145].

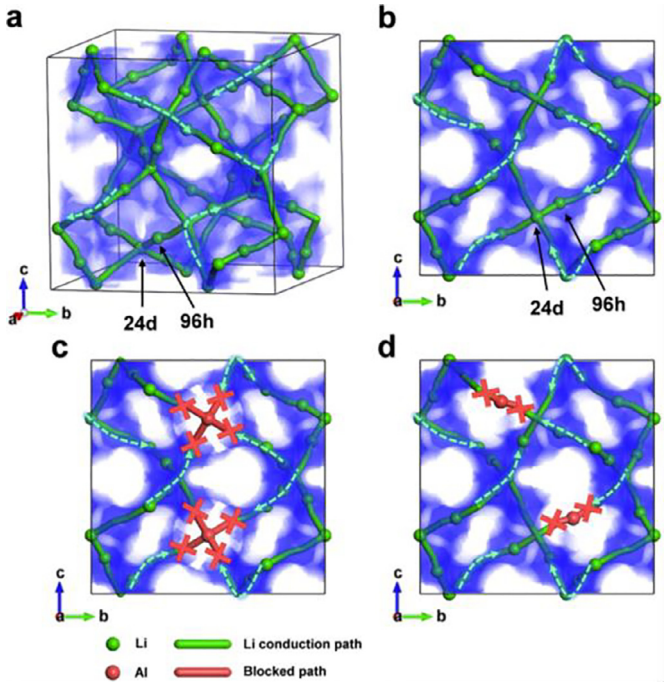

Fig. 7. Mulit-doping effect of on the Li ion diffusion in LLZO lattice (a) 3D image of the undoped cubic LLZO structure with two important sites of 24d and 96 h on the diffusion way of Li ion; (b) Projection of (a) along the [100] direction; (c) Al atom occupying the 24d site; and (d) Al atom occupying the 96 h site in case of co-doping of Ta (Reproduced from Shin et al.) [143].

In addition to the effort in improving the bulk of LLZO electrolyte, reducing interface impedance via formation of a conformal contact between the LLZO and electrode has also shown promising to improve the electrochemical performance of solid electrolyte as well. So far, deposition of a Si thin film via PECVD [146] and Ge by ALD technology [147] and preparation of a graphite surface layer by scratch with pencil [148] are performed to reduce the interfacial impedance between solid electrolyte and cathode particles. An extremely low interface impedance of 1Ω•cm [2] has been achieved in LLZO materials via ALD deposition of Al_2O_3 from the original 1710 Ω•cm [2,149]. It was believed that the conformal contact between solid-state electrolyte and Li metal, the enhanced interfacial kinetics due to thermally lithiated Al_2O_3 and the inhibition of Al_2O_3 against the formation of Li_2CO_3 are all ascribed to the ALD deposited thin film on the surface of LLZO. It was also found that sputtering of a thin layer of Au on the LLZO surface helped to suppress the growth of Lithium dendrites during high current cycling of all-solid-state lithium-ion batteries with Li foil as anode [150,151].

A series of researches for clarifying the influence of grain size, surface composition and air stability of LLZO has been carried out by Lei Cheng et al, and they found that interfacial impedance of the solid electrolyte has a critical relationship with their preparation history, and the particle size, surface state of particles and so on [152–155].

A very recent work is using an interphase $Li_{2.3-x}C_{0.7+x}B_{0.3-x}O_3$ to coating both solid electrolyte and cathode particles to realize an all-ceramic lithium-ion battery with high electrochemical performance. Here the natural impurity surface layer of LLZO due to contact with moisture in the air is no longer a problem, but an intended strategy. Fig. 8 shows the schematics of forming such an interphase between particles of LLZO electrolyte and LCO [156].

To build a 3D solid electrolyte scaffold structure, a ultra-fast high temperature sintering strategy was successfully developed in $Li_{6.5}La_3Zr_{1.5}Ta_{0.5}O_{12}$ (LLZTO) system as a demo, where thin porous

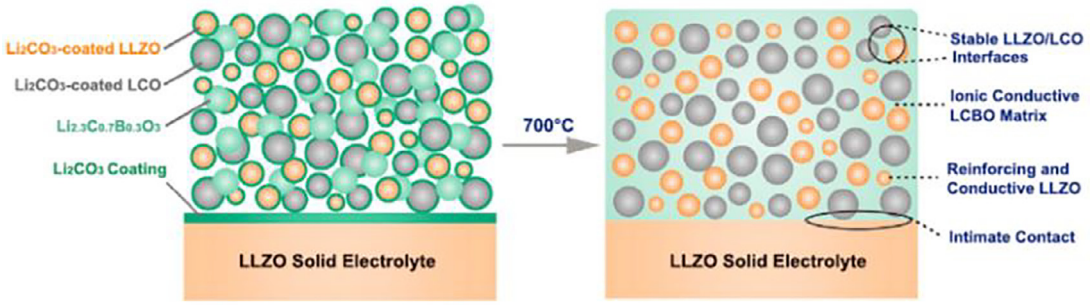

Fig. 8. Schematics of the interphase-engineered all-ceramic cathode/electrolyte (reproduced from Han et al.) [156].

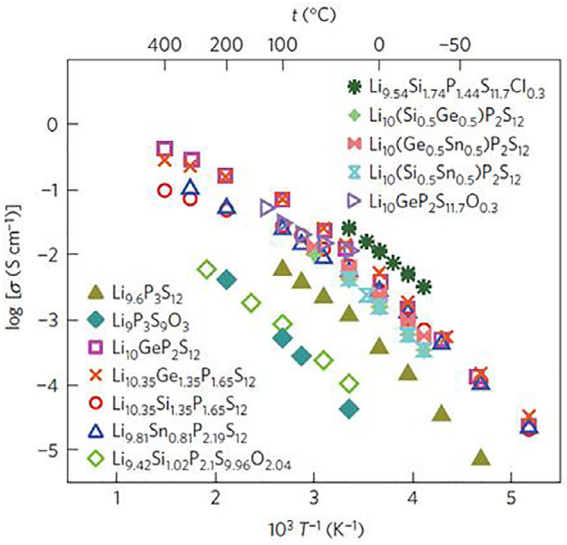

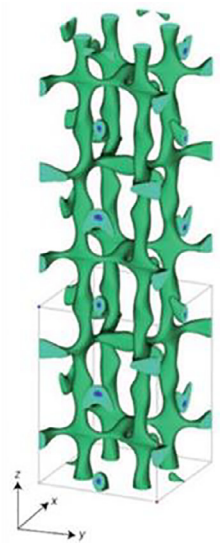

Fig. 9. Lithium-ion conductivity of LGPS family (a) and the nuclear distributions of Li atoms in $Li_{9.54}Si_{1.74}P_{1.44}S_{11.7}C_{l0.3}$ at 25 °C calculated using maximal entropy method (b) (reproduced from Kato et al.) [159].

LLZTO plate of 6μm can be sintered in seconds and shows a high ionic conductivity of ~7.3×10^{-4}S/cm [157].

2.5.2. (Thio-) LISICON structured sulfide electrolytes

Lithium sulfides have shown the highest Li ionic conductivity(≥ 1 mS/cm) in the family of inorganic electrolytes for lithium-ion batteries, which is comparable with that of liquid electrolyte, and have been treated as the promising solid electrolyte for lithium-ion batteries.

The first LISICON structured electrolyte $Li_{10}GeP_2S_{12}$ was reported by Kamaya *et al* to have a Li ionic conductivity as high as 12 mS/cm at room temperature [158]. Fig. 9 shows the comparison of Li ionic conductivity of different solid electrolytes. Their further researches on this LISICON structured sulfide solid electrolyte have resulted double the highest Li ionic conductivity of LISICON structured electrolyte to 25 mS/cm at room temperature through partial replacement of sulfur with some chlorine [159]. A widely distributed 3D conduction pathway was postulated in this material via calculation of maximum entropy method, which was ascribed to the high Li ionic conductivity as shown in Fig. 9(b). Their discovery also proves the applicability of sulfide electrolytes for the development of all solid-state lithium-ion batteries both with high voltage and high current capability, which shows potential for the development of automotive cells with high energy density and high-power densities.

To reduce the interfacial impedance between LISICON electrolyte and electrode, Sakuda et al. have performed a PLD deposition process to coat Li_2S-P_2S_5 onto the surface of LCO to enhance its surface electrochemical activity [160]. As shown in Fig. 10, a remarkable decrease of interfacial impedance at the solid-solid interface between solid cathode and sulfide electrolyte has been measured, and an improved rate capability has been achieved with this coated cathode strategy. Kim et al. have designed a solution processable solid electrolytes through mixing LiPSCl/EtOH (Ethanol) and LiT-Li_4SnS_4/MeOH (methanol) to prepare a fluid composite, then applied it to the as-prepared cathode film to fill the liquid electrolyte mixture into the porous cathodes, and the composite was then densified with cold pressing after removal of solvent to build a 3D interface between solid electrolyte and cathode [161]. Fig. 11 shows the schematic view of the innovative process for preparing all-solid-state lithium-ion batteries with conventional electrodes. To investigate its electrochemical stability window, first principle calculation has been carried out to found that $Li_{10}GeP_2S_{12}$ has a narrow electrochemical window against Li metal for application in all-solid-state Lithium-ion batteries and that a desired SEI phase formed spontaneously or artificially intended is crucial for its application in all-solid-state lithium-ion batteries [83]. The major challenge during the processing of sulfide electrolytes is that the LISICON compounds are extremely sensitive to moisture in the environment [162]. This imposes a very strict control of the water content of the atmosphere of the processing facilities.

In a very recent trial, a new design of a multilayer structure in which a less-stable electrolyte layer was sandwiched between two more-stable solid electrolyte layers, which prevented any lithium dendrite growth through well localized decompositions in the less stable electrolyte layer. A successfully demonstration was realized in the $Li_{5.5}PS_{4.5}Cl_{1.5}$–$Li_{9.54}Si_{1.74}(P_{0.9}Sb_{0.1})_{1.44}S_{11.7}Cl_{0.3}$–$Li_{5.5}PS_{4.5}Cl_{1.5}$ configuration, although this strategy should apply to other solid electrolyte systems [136].

2.5.3. NASICON structured electrolytes

The first report of high Li ionic conductivity up to 1.3 mS/cm at room temperature was reported by Jie Fu in 1997, which showed that a glass-ceramic composition of $14Li_2O$-$9Al_2O_3$-$38TiO_2$-$39P_2O_5$ could form a

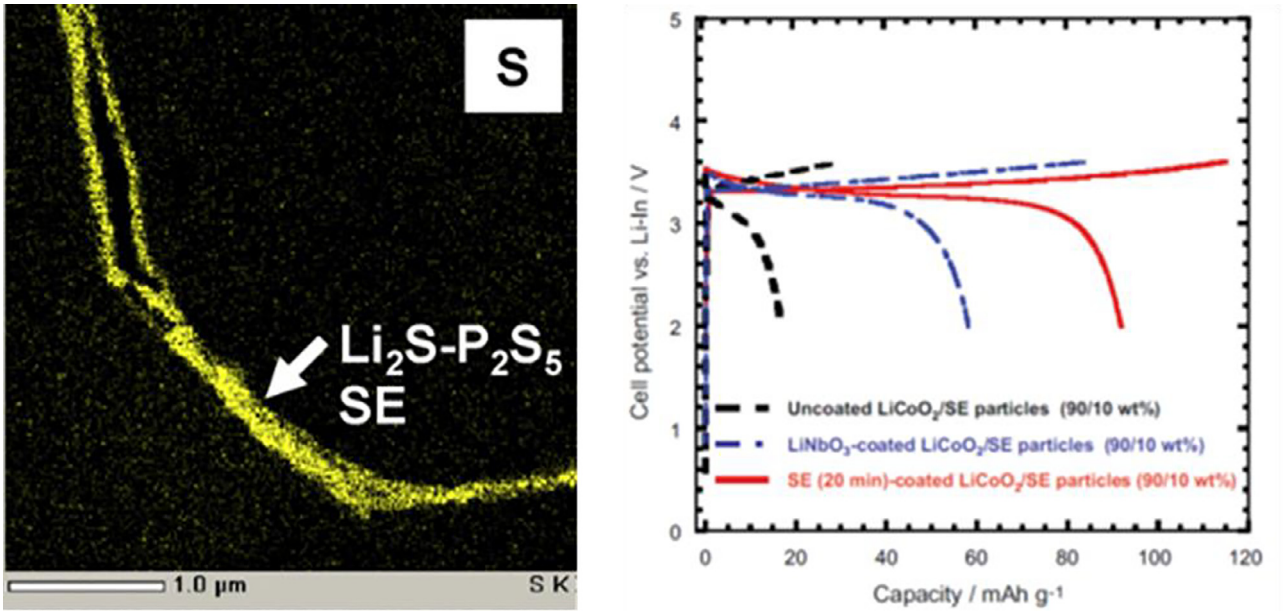

Fig. 10. PLD coated LCO (a) mapping S element at the boundary of particles and (b) the improved discharging performance (Reproduced from Sakuda et al.) [160].

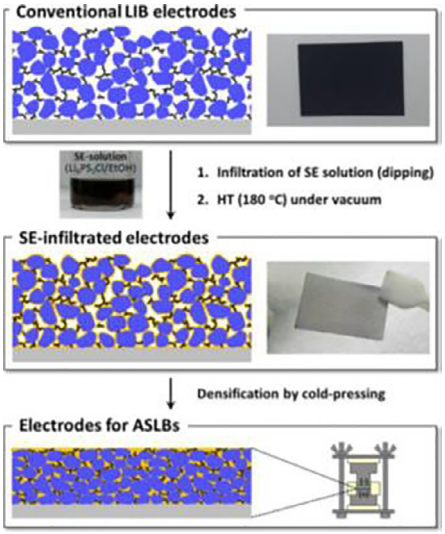

Fig. 11. Schematic diagram showing the process of filling the conventional electrode with solid electrolyte to prepare all-solid-state lithium-ion batteries (reproduced from Kim et al.) [161].

glass phase after thermal treatment at temperature as high 900 °C [163]. After that, a series of compositions of $Li_{1+x}Al_xTi_{2-x}(PO_4)_3$ (abbreviated as LATP) has been developed with various x with the amorphous structure aiming at high Lithium-ionic conductivity and good process capability as well. They are also provided in the forms of glass-ceramic mixtures, which are both stable thermally up to 600 °C and against humidity. Those advantages make them ideal for the development of aqueous based slurry all-solid-state lithium-ion batteries. High Li ionic conductivity as high as 1mS/cm has been reported in a commercial product of LATP by Ohara Incorporation [164]. Due to its good manufacturability at high temperature, LATP glass-ceramics have found wide application in the development of all-solid-state lithium ion batteries with innovative structure of solid electrolytes. Moreover, the influence of bias on the Li ionic conductivity at the grain boundaries of LATP glass-ceramic powders was also investigated, which showed that a periodic energy barrier exists at the grain boundaries of LATP samples, which acts as a modulation to the influence of bias on the Li ionic conductivity at those positions, and a rough thickness of 7.5 nm of the grain boundary of LIC-GC glass was estimated [165].

A recent breakthrough was achieved by using hot-pressing method to fabricate thin LAGP solid electrolyte plate (60μm) and assemble it with a thicker $LiFePO_4$ cathode with a commercially compatible areal capacity of 1 mAh/cm^2 [166].

2.5.4. *Perovskite structured electrolytes*

$Li_{0.5}La_{0.5}TiO_3$ (LLTO) belongs to another kind of oxide electrolyte with the perovskite structure, where half of the Li ions at the A-site in the lattice was replaced with La ions to generate volumetric expansion of the lattice, which facilitates the diffusion of Li ions in the material. The influence of Li concentration, thermal history during preparation, and the heating temperature on the structure and Li ionic conductivity has been reviewed recently by Wu et al. [167].

Anisotropy of Li ionic conductivity was found in the single crystal $Li_xLa_{(1-x)/3}NbO_3$, where the Li ionic conductivity shows the highest value of 0.36mS/cm in the directions of [100] and [010], which was about 10 times higher than that in the directions of [001] when x varies between 0.06 to 0.11.[168]

It is interesting to observe the domain walls in the microstructure of Li-rich and Li-poor LLTO materials with the high resolution TEM images, and the correspondingly random or highly disordered structure near the domain wall in the Li-poor sample Fig. 12(b)[169] is ascribed to a high lattice strain developed in the Li-rich LLTO sample, which results in a high obstacle to Li ion diffusion in the vicinity of domain wall or grain boundaries, thus a lower Li ion mobility than that in the Li-rich sample as shown in Fig. 12 (c) [169].

Amorphous LLTO thin film has been deposited via PLD technique to prepare solid-state micro-batteries, a high Li ionic conductivity of 0.3 mS/cm was observed in a 1.2 μm thick LLTO film under optimized growth condition [170].

Tape-casting process has been applied to confirm its feasibility for mass production of LLTO solid electrolyte thin sheet (25 μm) for the development of all-solid-state Li-metal batteries, since thin film of LLTO electrolyte is crucial for reducing the resistance in all-solid-state Li-metal batteries [171].

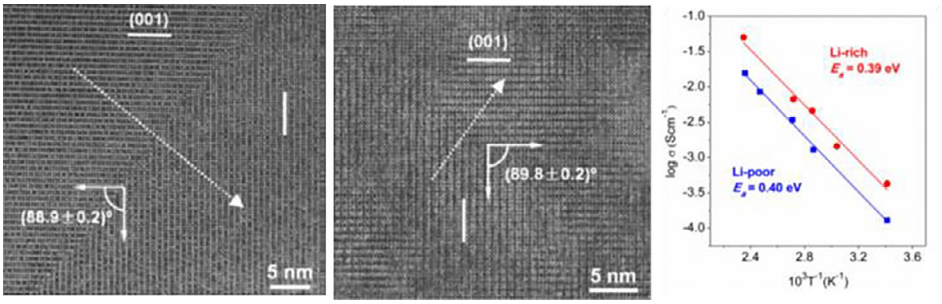

Fig. 12. High resolution lattice images of domain walls in (a) Li-rich and (b) Li-poor LLTO samples, (c) Li ion conductivity of Li- rich and poor LLTO material (reproduced from Gao et al.) [169].

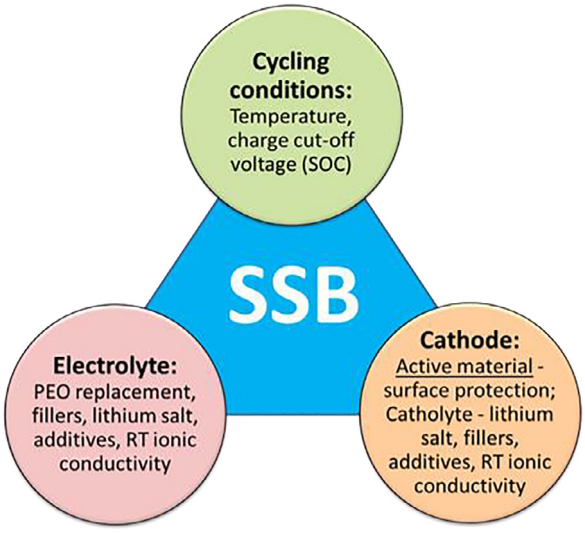

Fig. 13. Main factors affecting the electrochemical performance of a high voltage solid-state battery.

3. Outlook

The present review has provided a general outlook of the main classes of materials used as solid electrolytes in lithium ion and lithium metal batteries.

The classification done had the main scope to easily identify and select the best performing electrolytes for high voltage batteries, obtained with the help of a prism of performance representation (Fig. 13), summarized in Tables 3 –5.

Since the interpretation is quite complicated due to involvement of many factors, a simple correlation analysis was performed in order to reveal general trends and key factors that affect the electrochemical behavior of high voltage solid-state batteries with solid polymer and hybrid electrolytes. Fig. 14 depicts dependencies of capacity fade and factors such as: solid electrolyte type, operating temperature and charge voltage cut off.

Interestingly, a correlation between initial specific discharge cathode capacity and the logarithm of cell capacity fade was found for both solid electrolyte types (Fig. 14a). SSBs with hybrid solid electrolytes showed slightly lower dependence as a possible result of the whole system stabilization (dimensional, interfacial etc.). On the other hand, in accordance with Fig. 14b, increased operation temperature significantly deteriorates cycle life of solid-state batteries with SPEs whereas hybrid solid electrolytes-based ones appear more stable.

It is a well-known fact that charge cut off voltage is an important factor affecting electrochemical performance of SSBs. Here, we also found a clear tendency of capacity fade acceleration upon charge cut off voltage increase in case of SPEs as depicted in Fig. 14c. However, there is no strong correlation for all data sets in case of hybrid systems because many other factors like active material (Fig. 14c) electrolyte formulation, lithium salt (Fig. 14d) affect the electrochemical behavior.

Starting from the more traditional liquid electrolytes we tried to map the road towards SSBs, passing by the quasi-solid-state materials.

Among gel polymer electrolytes, PVdF based materials are among the most widespread. Research efforts have been brought to tailoring the microstructure by copolymerization processes and/or filler insertions, for the increasing of the amorphous phase, fundamental for the Lithium-ion conductivity. Conductivities in the order of 10^3 S/cm have been achieved.

Among the most promising materials we can mention PVDF/PAN 75:25 wt%, with electrochemical stability up to 5.1 V (vs LRE) and more than 90% capacity retention after 100 cycles. Also, other polymer-based materials have been developed, AMS (acrylonitrile-methyl methacrylate-styrene) is one of the most prominent technologies.

In this class also IGPEs materials deserve a mention. The implementation of ILs materials enables improved safety, along with good cyclability and high-capacity retention at room temperature.

The electrochemical stability range of solid electrolytes becomes essential for achieving high operating voltage in solid-state batteries [50]. Therefore, it is important to highlight that, despite many experimental works in the field of high voltage solid-state batteries, gaining in-depth fundamental understanding of mechanisms of the electrochemical decomposition and the development of a method for unambiguous electrochemical stability window determination is still strongly required [172].

On the other hand, testing in a real battery environment (assessing the effect of realistic usage profiles and of the impact of industrial processes on the performance of the full cell) is essential for better understanding of the relevance of the obtained experimental results.

The majority of gel electrolytes possess high ionic conductivity at room temperature due to the presence of a liquid phase embedded in the polymer matrix. Moreover, their electrochemical stability vs. Li/Li+ lithium reference electrode is mostly greater than 4.5 V. In addition to this, lithium-based batteries prepared with gel electrolytes provide better C-rate capability and coulombic efficiency, compared to truly all solid-state batteries.

Among solid polymer electrolytes, PEO based solid materials are nowadays the most widespread option. In its pure form PEO cannot guarantee great performances in terms of conductivities and electrochemical stabilities. Despite this, researchers have used PEO as a starting point for the creation of higher performance electrolytes, by copolymerization processes and using inorganic fillers.

Among solid inorganic electrolytes, (Thio-) LISICON seem to be able to guarantee the best performances in terms of voltage stability window (up to 5 V) and ionic conductivities, arriving also up to 25 mS/cm if partially doped, more than ten times higher if compared with the other solid inorganic materials (Garnet, NASICON, Perovskites).

4. Conclusions

To sum up, there is not one single solution to solve all existing problems related to high voltage stability. Nevertheless, several important

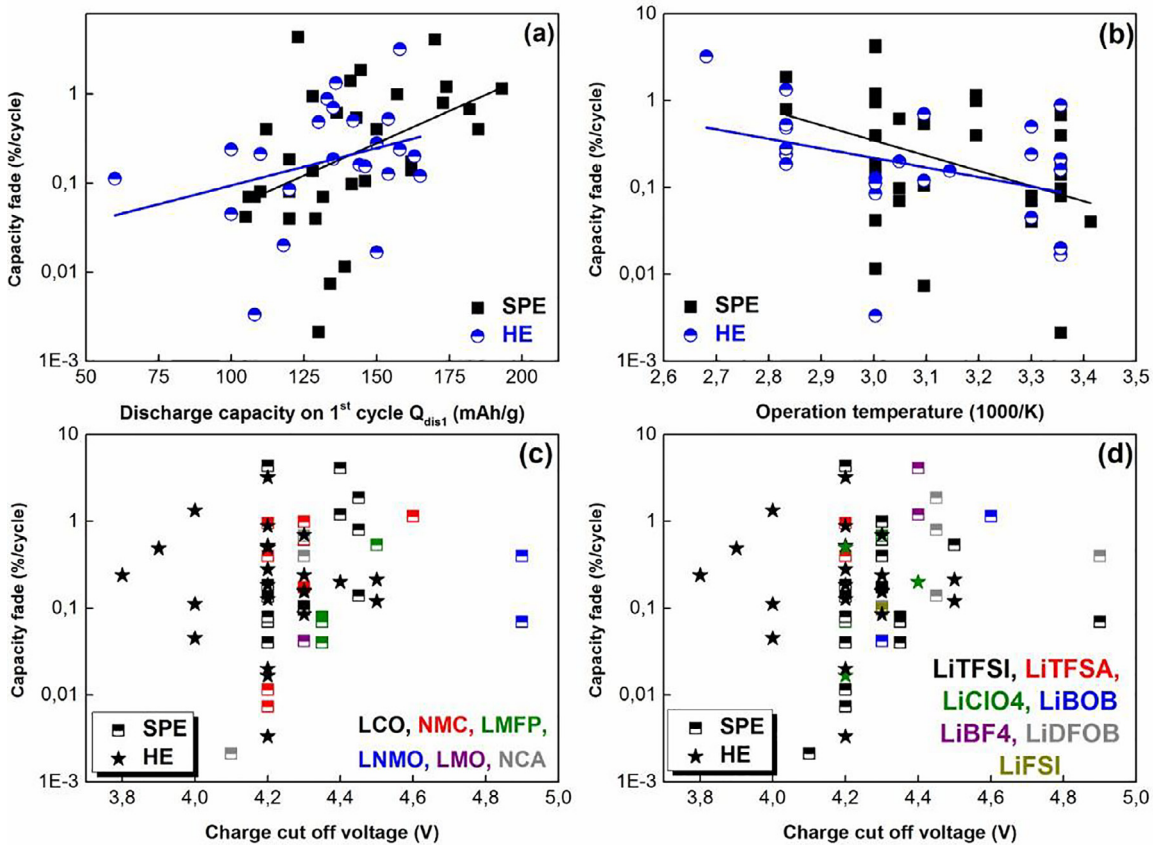

Fig. 14. Semilogarithmic dependences of capacity fade and initial discharge capacity (a); operation temperature (b); charge cut off voltage-color is function of cathode material (c), and lithium salt type in solid electrolyte (d) of solid-state batteries with solid polymer and hybrid electrolytes. Note: It should be noted that these figures do not gather information about all described above solid and hybrid electrolyte systems.

findings, which favor the development of better high voltage solid state battery, have been identified and summarized as follows:

(1) **Solid electrolyte:**
- Partial or full replacement PEO and its derivatives by novel polymers, plastic crystals, ionic liquids and inorganic materials (inert and conductive).
- Replacement of Lithium bis(trifluoromethanesulfonyl)imide by advanced lithium salts (lithium bis(oxalato)borate, Lithium difluoro(oxalato)borate, etc. and so on).
- Multilayered solid electrolyte design [173].
- Surface protection of solid electrolyte membranes.

(2) **High voltage positive electrode:**
- Surface protection of cathode materials [174,175].
- Functional additives to improve high voltage stability of catholyte (inorganic fillers, antioxidants, plasticizers, binders [176].

(3) **Cell Operation:**
- Lower operating temperature.
- Lower charge cut-off.

Finally, although authors mostly discussed existing technical challenges and opportunities in this thematic review, it will be equally important to put more focused effort on sustainable materials and production technology in the frame of the modern concepts of circular economy.

Declaration of Competing Interest

The authors declare that they have no known competing financial interests or personal relationships that could have appeared to influence the work reported in this paper.

All authors confirm that there is no conflict of interest.

Acknowledgment

The authors would like to thank the eCaiman project which was generously co-funded under the H2020 framework program by the European Union (Contract No.: 653331).

References

[1] Chen H, Cong TN, Yang W, Tan C, Li Y, Ding Y. Progress in electrical energy storage system: a critical review. Prog Nat Sci 2009;19:291–312.
[2] Luo X, Wang J, Dooner M, Clarke J. Overview of current development in electrical energy storage technologies and the application potential in power system operation. Appl Energy 2015;137:511–36.
[3] Blomgren GE. The development and future of lithium ion batteries. J Electrochem Soc 2016;164:A5019–25.
[4] Janek J, Zeier WG. A solid future for battery development. Nat Energy 2016;1:16141.
[5] Tan S, Ji YJ, Zhang ZR, Yang Y. Recent progress in research on high-voltage electrolytes for lithium-ion batteries. ChemPhysChem 2014;15:1956–69.
[6] Goodenough JB, Abruña HD, Buchanan MV. Basic Research Needs for Electrical Energy Storage. Report of the Basic Energy Sciences Workshop on Electrical Energy Storage 2007. doi:10.2172/935429.
[7] Goodenough JB, Park K-S. The Li-Ion rechargeable battery: a perspective. J Am Chem Soc 2013;135:1167–76.
[8] Peljo P, Girault HH. Electrochemical potential window of battery electrolytes: the homo–lumo misconception. Energy Environ Sci 2018;11:2306–9.
[9] Cheng F, Liang J, Tao Z, Chen J. Functional materials for rechargeable batteries. Adv Mater 2011;23:1695–715.

[10] Hu M, Pang X, Zhou Z. Recent progress in high-voltage lithium ion batteries. J Power Sources 2013;237:229–42.
[11] Kim JH, Pieczonka NPW, Yang L. Challenges and approaches for high-voltage spinel lithium-ion batteries. ChemPhysChem 2014;15:1940–54.
[12] Fey GTK, Li W, Dahn JR. Linivo4: A 4.8 Volt electrode material for lithium cells. J Electrochem Soc 1994;141:2279–82.
[13] Amine K, Yasuda H, Yamachi M. Olivine Licopo4 as 4.8 V electrode material for lithium batteries. Electrochem Solid State Lett 2000;3:178–9.
[14] Padhi AK, Nanjundaswamy KS, Goodenough JB. Phospho-olivines as positive-electrode materials for rechargeable lithium batteries. J Electrochem Soc 1997;144:1188–94.
[15] Markevich E, Salitra G, Aurbach D. Fluoroethylene carbonate as an important component for the formation of an effective solid electrolyte interphase on anodes and cathodes for advanced Li-Ion batteries. ACS Energy Lett 2017;2:1337–45.
[16] Wu B, Xu H, Mu D, Shi L, Jiang B, Gai L, Wang L, Liu Q, Ben L, Wu F. Controlled solvothermal synthesis and electrochemical performance of Licopo4 submicron single crystals as a cathode material for lithium ion batteries. J Power Sources 2016;304:181–8.
[17] Wang F, Yang J, NuLi Y, Wang J. Novel hedgehog-like 5v Licopo4 positive electrode material for rechargeable lithium battery. J Power Sources 2011;196:4806–10.
[18] Tussupbayev R, Taniguchi I. Physical and electrochemical properties of Licopo4/C nanocomposites prepared by a combination of emulsion drip combustion and wet ball-milling followed by heat treatment. J Power Sources 2013;236:276–84.
[19] Di Lecce D, Manzi J, Vitucci FM, De Bonis A, Panero S, Brutti S. Effect of the iron doping in Licopo4 cathode materials for lithium cells. Electrochim Acta 2015;185:17–27.
[20] Wang Y, Chen J, Qiu J, Yu Z, Ming H, Li M, Zhang S, Yang Y. Cr-substituted Licopo4 core with a conductive carbon layer towards high-voltage lithium-ion batteries. J Solid State Chem 2018;258:32–41.
[21] Ehrenberg H, Bramnik NN, Senyshyn A, Fuess H. Crystal and magnetic structures of electrochemically delithiated Li1−Xcopo4 phases. Solid State Sci 2009;11:18–23.
[22] Ikuhara YH, Gao X, Fisher CAJ, Kuwabara A, Moriwake H, Kohama K, Iba H, Ikuhara Y. Atomic level changes during capacity fade in highly oriented thin films of cathode material Licopo4. J Mater Chem A 2017;5:9329–38.
[23] Markevich E, Salitra G, Fridman K, Sharabi R, Gershinsky G, Garsuch A, Semrau G, Schmidt MA, Aurbach D. Fluoroethylene carbonate as an important component in electrolyte solutions for high-voltage lithium batteries: role of surface chemistry on the cathode. Langmuir 2014;30:7414–24.
[24] Liu X, Li D, Mo Q, Guo X, Yang X, Chen G, Zhong S. Facile synthesis of aluminum–DopedLini0.5mn1.5o4 hollow microspheres and their electrochemical performance for high-voltage Li-Ion batteries. J Alloys Compound 2014;609:54–9.
[25] Ue M, Sasaki Y, Tanaka Y, Morita M. Nonaqueous electrolytes with advances in solvents. In: Electrolytes for Lithium and Lithium-Ion Batteries. Springer; 2014. p. 93–165.
[26] Erickson EM, Markevich E, Salitra G, Sharon D, Hirshberg D, de la Llave E, Shterenberg I, Rosenman A, Frimer A, Aurbach D. Review-development of advanced rechargeable batteries: a continuous challenge in the choice of suitable electrolyte solutions. J Electrochem Soc 2015;162:A2424–38.
[27] Pham HQ, Lee HY, Hwang EH, Kwon YG, Song SW. Non-flammable organic liquid electrolyte for high-safety and high-energy density Li-Ion batteries. J Power Sources 2018;404:13–19.
[28] Wietelmann U, Bonrath W, Netscher T, Nöth H, Panitz J-C, Wohlfahrt-Mehrens M. Tris(Oxalato)phosphorus acid and its lithium salt. Chem A Eur J 2004;10:2451–8.
[29] Jiang Z, Carroll B, Abraham KM. Studies of some poly(Vinylidene Fluoride) electrolytes. Electrochim Acta 1997;42:2667–77.
[30] Miao R, Liu B, Zhu Z, Liu Y, Li J, Wang X, Li Q. Pvdf-Hfp-based porous polymer electrolyte membranes for lithium-ion batteries. J Power Sources 2008;184:420–6.
[31] Kim KM, Ryu KS, Kang SG, Chang SH, Chung IJ. The effect of silica addition on the properties of poly((Vinylidene Fluoride)-co-hexafluoropropylene)-based polymer electrolytes. Macromol Chem Phys 2001;202:866–72.
[32] Gopalan A, Santhosh P, Manesh K, Nho J, Kim S, Hwang C, Lee K. Development of electrospun pvdf–pan membrane-based polymer electrolytes for lithium batteries. J Membr Sci 2008;325:683–90.
[33] Periasamy P, Tatsumi K, Shikano M, Fujieda T, Saito Y, Sakai T, Mizuhata M, Kajinami A, Deki S. Studies on Pvdf-based gel polymer electrolytes. J Power Sources 2000;88:269–73.
[34] Zhang HP, Zhang P, Li GC, Wu YP, Sun DL. A porous poly(Vinylidene Fluoride) gel electrolyte for lithium ion batteries prepared by using salicylic acid as a foaming agent. J Power Sources 2009;189:594–8.
[35] Lombardo L, Navarra MA, Panero S, Medina LA, Matic A, Hassoun J. *In-Situ* gelled electrolyte for lithium battery: electrochemical and raman characterization. J Power Sources 2014;245:232–5.
[36] Song MK, Cho JY, Cho BW, Rhee HW. Characterization of Uv-cured gel polymer electrolytes for rechargeable lithium batteries. J Power Sources 2002;110:209–15.
[37] Gopalan AI, Santhosh P, Manesh KM, Nho JH, Kim SH, Hwang CG, Lee KP. Development of electrospun Pvdf–pan membrane-based polymer electrolytes for lithium batteries. J Membr Sci 2008;325:683–90.
[38] Xing Y, Wu Y, Wang H, Yang G, Li W, Xu L, Jiang X. Preparation of hybrid polymer based on polyurethane lithium salt and polyvinylidene fluoride as electrolyte for lithium-ion batteries. Electrochim Acta 2014;136:513–20.
[39] Jamalpour S, Ghahramani M, Ghaffarian SR, Javanbakht M. The effect of poly(Hydroxyl Ethyl Methacrylate) on the performance of Pvdf/P(Mma-Co-Hema) hybrid gel polymer electrolytes for lithium ion battery application. Polymer 2020;195:122427.
[40] Cheng CL, Wan CC, Wang YY. Preparation of porous, chemically cross-linked, pvdf-based gel polymer electrolytes for rechargeable lithium batteries. J Power Sources 2004;134:202–10.
[41] Croce F, Focarete ML, Hassoun J, Meschini I, Scrosati B, Safe A. High-rate and high-energy polymer lithium-ion battery based on gelled membranes prepared by electrospinning. Energy Environ Sci 2011;4:921–7.
[42] Zhang J, Liu Z, Kong Q, Zhang C, Pang S, Yue L, Wang X, Yao J, Cui G. Renewable and superior thermal-resistant cellulose-based composite nonwoven as lithium-ion battery separator. ACS Appl Mater Interfaces 2013;5:128–34.
[43] Liang YF, Xia Y, Zhang SZ, Wang XL, Xia XH, Gu CD, Wu JB, Tu JP. A preeminent gel blending polymer electrolyte of poly(Vinylidene Fluoride-Hexafluoropropylene) -poly(Propylene Carbonate) for solid-state lithium ion batteries. Electrochim Acta 2019;296:1064–9.
[44] Kim DW, Sun YK. Effect of mixed solvent electrolytes on cycling performance of rechargeable Li/Lini0.5co0.5o2 cells with gel polymer electrolytes. Solid State Ionics 1998;111:243–52.
[45] Zhao J, et al. A sustainable and rigid-flexible coupling cellulose-supported poly(propylene carbonate) polymer electrolyte towards 5 V high voltage lithium batteries. Electrochim Acta 2016;188:23–30.
[46] Dong T, et al. A multifunctional polymer electrolyte enables ultra-long cycle-life in a high-voltage lithium metal battery. Energy Environ Sci 2018;11:1197–203.
[47] Ye F, Zhang X, Liao K, Lu Q, Zou X, Ran R, Zhou W, Zhong Y, Shao Z. A smart lithiophilic polymer filler in gel polymer electrolyte enables stable and dendrite-free Li metal anode. J Mater Chem A 2020;8:9733–42.
[48] Zhou YF, Xie S, Ge XW, Chen CH, Amine K. Preparation of rechargeable lithium batteries with poly(methyl methacrylate) based gel polymer electrolyte by *in situ* γ-ray irradiation-induced polymerization. J Appl Electrochem 2004;34:1119–25.
[49] Chai J, Liu Z, Ma J, Wang J, Liu X, Liu H, Zhang J, Cui G, Chen L. *In Situ* generation of poly (vinylene carbonate) based solid electrolyte with interfacial stability for Licoo2 lithium batteries. Adv Sci 2017;4:1600377 (Weinh).
[50] Chai J, Liu Z, Zhang J, Sun J, Tian Z, Ji Y, Tang K, Zhou X, Cui G. A superior polymer electrolyte with rigid cyclic carbonate backbone for rechargeable lithium ion batteries. ACS Appl Mater Interfaces 2017;9:17897–905.
[51] Cui Y, Chai J, Du H, Duan Y, Xie G, Liu Z, Cui G. Facile and reliable *in situ* polymerization of poly(Ethyl Cyanoacrylate)-based polymer electrolytes toward flexible lithium batteries. ACS Appl Mater Interfaces 2017;9:8737–41.
[52] Liu X, Ding G, Zhou X, Li S, He W, Chai J, Pang C, Liu Z, Cui G. An interpenetrating network poly(diethylene glycol carbonate)-based polymer electrolyte for solid-state lithium batteries. J Mater Chem A 2017;5:11124–30.
[53] Li X, et al. A dual-functional gel-polymer electrolyte for lithium ion batteries with superior rate and safety performances. J Mater Chem A 2017;5:18888–95.
[54] Ma Y, et al. Two players make a formidable combination: *in situ* generated poly(acrylic anhydride-2-methyl-acrylic acid-2-oxirane-ethyl ester-methyl methacrylate) cross-linking gel polymer electrolyte toward 5 V high-voltage batteries. ACS Appl Mater Interfaces 2017;9:41462–72.
[55] Karuppasamy K, Reddy PA, Srinivas G, Tewari A, Sharma R, Shajan XS, Gupta D. Electrochemical and cycling performances of novel nonafluorobutanesulfonate (nonaflate) ionic liquid based ternary gel polymer electrolyte membranes for rechargeable lithium ion batteries. J Membr Sci 2016;514:350–7.
[56] Karuppasamy K, Reddy PA, Srinivas G, Sharma R, Tewari A, Kumar GH, Gupta D. An efficient way to achieve high ionic conductivity and electrochemical stability of safer nonaflate anion-based ionic liquid gel polymer electrolytes (ilgpes) for rechargeable lithium ion batteries. J Solid State Electrochem 2016;21:1145–55.
[57] Karuppasamy K, Kim HS, Kim D, Vikraman D, Prasanna K, Kathalingam A, Sharma R, Rhee HW. An enhanced electrochemical and cycling properties of novel boronic ionic liquid based ternary gel polymer electrolytes for rechargeable Li/Licoo2 cells. Sci Rep 2017;7:11103.
[58] Balo L, Gupta H, Singh SK, Singh VK, Tripathi AK, Srivastava N, Tiwari RK, Mishra R, Meghnani D, Singh RK. Development of gel polymer electrolyte based on litfsi and emimfsi for application in rechargeable lithium metal battery with Go-Lfp and Nca cathodes. J Solid State Electrochem 2019;23:2507–18.
[59] Singh SK, Dutta D, Singh RK. Enhanced structural and cycling stability of Li_2CuO_2-coated $Lini_{0.33}MN_{0.33}CO_{0.33}O_2$ cathode with flexible ionic liquid-based gel polymer electrolyte for lithium polymer batteries. Electrochim Acta 2020;343:136122.
[60] Srivastava N, Singh SK, Gupta H, Meghnani D, Mishra R, Tiwari RK, Patel A, Tiwari A, Singh RK. Electrochemical performance of Li-Rich Nmc cathode material using ionic liquid based blend polymer electrolyte for rechargeable Li-Ion batteries. J Alloys Compound 2020;843:155615.
[61] Armand M, Chabagno J, Duclot M. Fast ion transport in solids. Polyethers as solid electrolytes 1979:131–6.
[62] Hovington P, Lagace M, Guerfi A, Bouchard P, Mauger A, Julien CM, Armand M, Zaghib K. New lithium metal polymer solid state battery for an ultrahigh energy: nano C-LiFePo$_4$ versus nano $Li_{1.2}V_3O_8$. Nano Lett 2015;15:2671–8.
[63] Perea A, Dontigny M, Zaghib K. Safety of solid-state li metal battery: solid polymer versus liquid electrolyte. J Power Sources 2017;359:182–5.
[64] Blue Solution-Bollere Group. https://www.blue-solutions.com/en/blue-solutions/technology/batteries-lmp/.
[65] Zhou Q, Zhang J, Cui G. Rigid–flexible coupling polymer electrolytes toward high-energy lithium batteries. Macromol Mater Eng 2018:303.
[66] Nitta N, Wu F, Lee JT, Yushin G. Li-ion battery materials: present and future. Mater Today 2015;18:252–64.
[67] Goodenough JB, Kim Y. Challenges for rechargeable Li batteries†. Chem Mater 2010;22:587–603.
[68] Placke T, Kloepsch R, Dühnen S, Winter M. Lithium ion, lithium metal, and alternative rechargeable battery technologies: the odyssey for high energy density. J Solid State Electrochem 2017;21:1939–64.

[69] Keller M, Varzi A, Passerini S. Hybrid electrolytes for lithium metal batteries. J Power Sources 2018;392:206–25.
[70] Bouchet R, Maria S, Meziane R, Aboulaich A, Lienafa L, Bonnet JP, Phan TN, Bertin D, Gigmes D, Devaux D. Single-ion bab triblock copolymers as highly efficient electrolytes for lithium-metal batteries. Nat Mater 2013;12:452–7.
[71] Porcarelli L, Gerbaldi C, Bella F, Nair JR. Super Soft all-ethylene oxide polymer electrolyte for safe all-solid lithium batteries. Sci Rep 2016;6:19892.
[72] Yue L, Ma J, Zhang J, Zhao J, Dong S, Liu Z, Cui G, Chen L. All solid-state polymer electrolytes for high-performance lithium ion batteries. Energy Storage Mater 2016;5:139–64.
[73] Xue Z, He D, Xie X. Poly(ethylene oxide)-based electrolytes for lithium-ion batteries. J Mater Chem A 2015;3:19218–53.
[74] Mindemark J, Lacey MJ, Bowden T, Brandell D. Beyond peo-alternative host materials for Li+-conducting solid polymer electrolytes. Prog Polym Sci 2018;81:114–43.
[75] Ma J, Liu Z, Chen B, Wang L, Yue L, Liu H, Zhang J, Liu Z, Cui G. A strategy to make high voltage licoo2 compatible with polyethylene oxide electrolyte in all-solid-state lithium ion batteries. J Electrochem Soc 2017;164:A3454–61.
[76] Yao P, et al. Pvdf/palygorskite nanowire composite electrolyte for 4 V rechargeable lithium batteries with high energy density. Nano Lett 2018;18:6113–20.
[77] Li Q, Takeda Y, Imanish N, Yang J, Sun H, Yamamoto O. Cycling performances and interfacial properties of a Li/Peo-Li (CF_3SO_2) 2n-ceramic filler/$Lini_{0.8}CO_{0.2}O_2$ Cell. J Power Sources 2001;97:795–7.
[78] Li Q, Imanishi N, Hirano A, Takeda Y, Yamamoto O. Four volts class solid lithium polymer batteries with a composite polymer electrolyte. J Power Sources 2002;110:38–45.
[79] Wetjen M, Kim G-T, Joost M, Appetecchi GB, Winter M, Passerini S. Thermal and electrochemical properties of peo-litfsi-pyr14tfsi-based composite cathodes, incorporating 4 v-class cathode active materials. J Power Sources 2014;246:846–57.
[80] Jung YC, Park MS, Kim DH, Ue M, Eftekhari A, Kim DW. Room-temperature performance of poly(ethylene ether carbonate)-based solid polymer electrolytes for all-solid-state lithium batteries. Sci Rep 2017;7:17482.
[81] Ma J, Chen B, Wang L, Cui G. Progress and prospect on failure mechanisms of solid-state lithium batteries. J Power Sources 2018;392:94–115.
[82] Faglioni F, Merinov BV, Goddard WA, Kozinsky B. Factors affecting cyclic durability of all-solid-state lithium batteries using poly (ethylene oxide)-based polymer electrolytes and recommendations to achieve improved performance. Phys Chem Chem Phys 2018;20:26098–104.
[83] Han F, Zhu Y, He X, Mo Y, Wang C. Electrochemical stability of $Li_{10}GEP_2S_{12}$ and $Li_7La_3Zr_2O_{12}$ solid electrolytes. Adv Energy Mater 2016;6:1501590.
[84] Hallinan TD Jr, Rausch A, McGill B. An electrochemical approach to measuring oxidative stability of solid polymer electrolytes for lithium batteries. Chemical Engin Sci 2016;154:34–41.
[85] Xia Y, Fujieda T, Tatsumi K, Prosini PP, Sakai T. Thermal and electrochemical stability of cathode materials in solid polymer electrolyte. J Power Sources 2001;92:234–43.
[86] Karthik K, Murugan R. Lithium garnet based free-standing solid polymer composite membrane for rechargeable lithium battery. J Solid State Electrochem 2018;22:2989–98.
[87] Manuel Stephan A, Nahm KS. Review on composite polymer electrolytes for lithium batteries. Polymer 2006;47:5952–64.
[88] Zhang Q, Liu K, Ding F, Liu X. Recent advances in solid polymer electrolytes for lithium batteries. Nano Res 2017;10:4139–74.
[89] Commarieu B, Paolella A, Daigle JC, Zaghib K. Toward high lithium conduction in solid polymer and polymer–ceramic batteries. Curr Op Electrochem 2018;9:56–63.
[90] Zhao Q, Stalin S, Zhao CZ, Archer LA. Designing solid-state electrolytes for safe, energy-dense batteries. Nat Rev Mater 2020;5:229–52.
[91] Xiao Y, Wang Y, Bo SH, Kim JC, Miara LJ, Ceder G. Understanding interface stability in solid-state batteries. Nat Rev Mater 2020;5:105–26.
[92] Matsui S, Muranaga T, Higobashi H, Inoue S, Sakai T. Liquid-free rechargeable Li polymer battery. J Power Sources 2001;97-98:772–4.
[93] Kobayashi Y, Shono K, Kobayashi T, Ohno Y, Tabuchi M, Oka Y, Nakamura T, Miyashiro H. A long life 4 v class lithium-ion polymer battery with liquid-free polymer electrolyte. J Power Sources 2017;341:257–63.
[94] Seki S. Solvent-free 4 V-class all-solid-state lithium-ion polymer secondary batteries. ChemistrySelect 2017;2:3848–53.
[95] Takada K. Progress in solid electrolytes toward realizing solid-state lithium batteries. J Power Sources 2018;394:74–85.
[96] Seki S, Kobayashi Y, Miyashiro H, Mita Y, Iwahori T. Fabrication of high-voltage, high-capacity all-solid-state lithium polymer secondary batteries by application of the polymer electrolyte/inorganic electrolyte composite concept. Chem Mater 2005;17:2041–5.
[97] Yang Q, Huang J, Li Y, Wang Y, Qiu J, Zhang J, Yu H, Yu X, Li H, Chen L. Surface-protected Licoo2 with ultrathin solid oxide electrolyte film for high–voltage lithium ion batteries and lithium polymer batteries. J Power Sources 2018;388:65–70.
[98] Niitani T, Shimada M, Kawamura K, Kanamura K. Characteristics of new-type solid polymer electrolyte controlling nano-structure. J Power Sources 2005;146:386–90.
[99] Niitani T, Shimada M, Kawamura K, Dokko K, Rho YH, Kanamura K. Synthesis of Li^+ ion conductive peo-pst block copolymer electrolyte with microphase separation structure. Electrochem Solid State Lett 2005;8.
[100] Zhang J, et al. Taichi-inspired rigid-flexible coupling cellulose-supported solid polymer electrolyte for high-performance lithium batteries. Sci Rep 2014;4:6272.
[101] Zhang X, Wang S, Xue C, Xin C, Lin Y, Shen Y, Li L, Nan CW. Self-suppression of lithium dendrite in all-solid-state lithium metal batteries with poly(vinylidene difluoride)-based solid electrolytes. Adv Mater 2019;31:1806082.
[102] He W, Cui Z, Liu X, Cui Y, Chai J, Zhou X, Liu Z, Cui G. Carbonate-linked poly(ethylene oxide) polymer electrolytes towards high performance solid state lithium batteries. Electrochim Acta 2017;225:151–9.
[103] Zhang J, et al. Safety-reinforced poly(propylene carbonate)-based all-solid-state polymer electrolyte for ambient-temperature solid polymer lithium batteries. Advanced Energy Mater 2015;5(24):1501082.
[104] Liu J, Shen X, Zhou J, Wang M, Niu C, Qian T, Yan C. Nonflammable and high-voltage-tolerated polymer electrolyte achieving high stability and safety in 4.9 V-class lithium metal battery. ACS Appl Mater Interfaces 2019;11:45048–56.
[105] Polo Fonseca C, Neves S. Electrochemical properties of a biodegradable polymer electrolyte applied to a rechargeable lithium battery. J Power Sources 2006;159:712–16.
[106] Oh B, Vissers D, Zhang Z, West R, Tsukamoto H, Amine K. New interpenetrating network type poly(siloxane-g-ethylene oxide) polymer electrolyte for lithium battery. J Power Sources 2003;119-121:442–7.
[107] Liu M, Jin B, Zhang Q, Zhan X, Chen F. High-performance solid polymer electrolytes for lithium ion batteries based on sulfobetaine zwitterion and poly (ethylene oxide) modified polysiloxane. J Alloys Compound 2018;742:619–28.
[108] Abouimrane A, Davidson IJ. Solid electrolyte based on succinonitrile and Libob. J Electrochem Soc 2007;154:A1031.
[109] Choi KH, Cho SJ, Kim SH, Kwon YH, Kim JY, Lee SY. Thin, deformable, and safety-reinforced plastic crystal polymer electrolytes for high-performance flexible lithium-ion batteries. Adv Funct Mater 2014;24:44–52.
[110] Grundish NS, Goodenough JB, Khani H. Designing composite polymer electrolytes for all-solid-state lithium batteries. Curr Op Electrochem 2021.
[111] Chen H, Adekoya D, Hencz L, Ma J, Chen S, Yan C, Zhao H, Cui G, Zhang S. Stable seamless interfaces and rapid ionic conductivity of ca–ceo2/litfsi/peo composite electrolyte for high-rate and high-voltage all-solid-state battery. Adv Energy Mater 2020:10.
[112] Zhang S, Li Z, Guo Y, Cai L, Manikandan P, Zhao K, Li Y, Pol VG. Room-temperature, high-voltage solid-state lithium battery with composite solid polymer electrolyte with in-situ thermal safety study. Chem Eng J 2020;400:125996.
[113] Liu X, Li X, Li H, Wu HB. Recent progress of hybrid solid-state electrolytes for lithium batteries. Chemistry 2018;24:18293–306.
[114] Li Q, Itoh T, Imanishi N, Hirano A, Takeda Y, Yamamoto O. All solid lithium polymer batteries with a novel composite polymer electrolyte. Solid State Ionics 2003;159:97–109.
[115] Lin Y, Cheng Y, Li J, Miller JD, Liu J, Wang X. Biocompatible and biodegradable solid polymer electrolytes for high voltage and high temperature lithium batteries. RSC Adv 2017;7:24856–63.
[116] Wang S, Li J, Li Q, Chen J, Liu X, Wang Z, Zeng Q, Zhao T, Liu X, Zhang L. Topological polymer electrolyte containing poly(pinacol vinylboronate) segments composited with ceramic nanowires towards ambient-temperature superior performance all-solid-state lithium batteries. J Power Sources 2019;413:318–26.
[117] Zhao Y, Wu C, Peng G, Chen X, Yao X, Bai Y, Wu F, Chen S, Xu X. A new solid polymer electrolyte incorporating $Li_{10}GeP_2S_{12}$ into a polyethylene oxide matrix for all-solid-state lithium batteries. J Power Sources 2016;301:47–53.
[118] Choi JH, Lee CH, Yu JH, Doh CH, Lee SM. Enhancement of ionic conductivity of composite membranes for all-solid-state lithium rechargeable batteries incorporating tetragonal $LI_7La_3Zr_2O_{12}$ into a polyethylene oxide matrix. J Power Sources 2015;274:458–63.
[119] Zhang J, Zhao N, Zhang M, Li Y, Chu PK, Guo X, Di Z, Wang X, Li H. Flexible and ion-conducting membrane electrolytes for solid-state lithium batteries: dispersion of garnet nanoparticles in insulating polyethylene oxide. Nano Energy 2016;28:447–54.
[120] Karthik K, Murugan R. Flexible high Li+ conductive lithium garnet–based dry solid polymer electrolyte membrane with enhanced electrochemical performance for lithium metal batteries. Ionics 2019;25:4703–11.
[121] Xu H, Chien PH, Shi J, Li Y, Wu N, Liu Y, Hu YY, Goodenough JB. High-performance all-solid-state batteries enabled by salt bonding to perovskite in poly(ethylene oxide). Proc Natl Acad Sci 2019;116:18815–21.
[122] Zhang J, Zheng C, Lou J, Xia Y, Liang C, Huang H, Gan Y, Tao X, Zhang W. Poly(ethylene oxide) reinforced $Li_6Ps_5C_l$ composite solid electrolyte for all-solid-state lithium battery: enhanced electrochemical performance, mechanical property and interfacial stability. J Power Sources 2019;412:78–85.
[123] Zhao Q, Chen P, Li S, Liu X, Archer LA. Solid-state polymer electrolytes stabilized by task-specific salt additives. J Mater Chem A 2019;7:7823–30.
[124] Wang C, Yang Y, Liu X, Zhong H, Xu H, Xu Z, Shao H, Ding F. Suppression of lithium dendrite formation by using lagp-peo (litfsi) composite solid electrolyte and lithium metal anode modified by peo (litfsi) in all-solid-state lithium batteries. ACS Appl Mater Interfaces 2017;9:13694–702.
[125] Zhang J, et al. High-voltage and free-standing poly(propylene carbonate)/$Li_{6.75}La_3Zr_{1.75}Ta_{0.25}O_{12}$ composite solid electrolyte for wide temperature range and flexible solid lithium ion battery. J Mater Chem A 2017;5:4940–8.
[126] Park MS, Jung YC, Kim DW. Hybrid solid electrolytes composed of poly(1,4-butylene adipate) and lithium aluminum germanium phosphate for all-solid-state Li/$LiNi_{0.6}Co_{0.2}Mn_{0.2}O_2$ cells. Solid State Ionics 2018;315:65–70.
[127] Zhang X, Liu T, Zhang S, Huang X, Xu B, Lin Y, Xu B, Li L, Nan CW, Shen Y. Synergistic coupling between $Li_{6.75}La_3Zr_{1.75}Ta_{0.25}O_{12}$ and poly(vinylidene fluoride) induces high ionic conductivity, mechanical strength, and thermal stability of solid composite electrolytes. J Am Chem Soc 2017;139:13779–85.
[128] Jing M-x, Yang H, Chong H, Chen F, Zhang L-k, Hu X-y, Tu F-y, Shen X-q. Synergistic enhancement effects of llzo fibers and interfacial modification for polymer solid electrolyte on the ambient-temperature electrochemical performances of solid-state battery. J Electrochem Soc 2019;166:A3019–27.
[129] Kim HW, Manikandan P, Lim YJ, Kim JH, Nam SC, Kim Y. Hybrid solid electrolyte

with the combination of $Li_7La_3Zr_2O_{12}$ ceramic and ionic liquid for high voltage pseudo-solid-state Li-Ion batteries. J Mater Chem A 2016;4:17025–32.
[130] Choi H, Kim HW, Ki JK, Lim YJ, Kim Y, Ahn JH. Nanocomposite quasi-solid-state electrolyte for high-safety lithium batteries. Nano Res 2017;10:3092–102.
[131] Famprikis T, Canepa P, Dawson JA, Islam MS, Masquelier C. Fundamentals of inorganic solid-state electrolytes for batteries. Nat Mater 2019;18:1278–91.
[132] Park KH, Kaup K, Assoud A, Zhang Q, Wu X, Nazar LF. High-voltage superionic halide solid electrolytes for all-solid-state Li-Ion batteries. ACS Energy Lett 2020;5:533–9.
[133] Cheng Z, Zahiri B, Ji X, Chen C, Chalise D, Braun PV, Cahill DG. Good solid-state electrolytes have low, glass-like thermal conductivity. Small 2021:17.
[134] Ohno S, et al. How certain are the reported ionic conductivities of thiophosphate-based solid electrolytes? An interlaboratory study. ACS Energy Lett 2020;5:910–15.
[135] Kim KJ, Balaish M, Wadaguchi M, Kong L, Rupp JLM. Solid-state Li–metal batteries: challenges and horizons of oxide and sulfide solid electrolytes and their interfaces. Adv Energy Mater 2021;11:2002689.
[136] Ye L, Li X. A dynamic stability design strategy for lithium metal solid state batteries. Nature 2021;593:218–22.
[137] Bachman JC, et al. Inorganic solid-state electrolytes for lithium batteries: mechanisms and properties governing ion conduction. Chem Rev 2016;116:140–62.
[138] Jin Y, McGinn PJ. Al-doped $Li_7La_3Zr_2O_{12}$ synthesized by a polymerized complex method. J Power Sources 2011;196:8683–7.
[139] Rettenwander D, et al. Structural and electrochemical consequences of al and ga cosubstitution in $Li_{7l}A_3Zr_2O_{12}$ solid electrolytes. Chem Mater 2016;28:2384–92.
[140] Rettenwander D, Welzl A, Cheng L, Fleig J, Musso M, Suard E, Doeff MM, Redhammer GJ, Amthauer G. Synthesis, Crystal chemistry, and electrochemical properties of $Li_{7-2X}La_3Zr_{2-X}Mo_xO_{12}$ (X = 0.1–0.4): stabilization of the cubic garnet polymorph via substitution of Zr^{4+} by Mo^{6+}. Inorg Chem 2015;54:10440–9.
[141] Rettenwander D, Geiger CA, Tribus M, Tropper P, Wagner R, Tippelt G, Lottermoser W, Amthauer G. The Solubility and site preference of Fe^{3+} in $Li_{7-3x}Fe_xLa_3ZrO_{12}$ garnets. J Solid State Chem 2015;230:266–71.
[142] Wu JF, Chen EY, Yu Y, Liu L, Wu Y, Pang WK, Peterson VK, Guo X. Gallium-doped $Li_7La_3Zr_2O_{12}$ garnet-type electrolytes with high lithium-ion conductivity. ACS Appl Mater Interfaces 2017;9:1542–52.
[143] Shin DO, Oh K, Kim KM, Park KY, Lee B, Lee YG, Kang K. Synergistic multi-doping effects on the $Li_7La_3Zr_2O_{12}$ solid electrolyte for fast lithium ion conduction. Sci Rep 2015;5:18053.
[144] David IN, Thompson T, Wolfenstine J, Allen JL, Sakamoto J. Microstructure and Li-ion conductivity of hot-pressed cubic $Li_7La_3Zr_2O_{12}$. J Am Ceram Soc 2015;98:1209–14.
[145] Shin RH, Son SI, Han YS, Kim YD, Kim HT, Ryu SS, Pan W. Sintering behavior of garnet-type $Li_7La_3Zr_2O_{12}$-Li_3Bo_3 composite solid electrolytes for all-solid-state lithium batteries. Solid State Ionics 2017;301:10–14.
[146] Luo W, et al. Transition from superlithiophobicity to superlithiophilicity of garnet solid-state electrolyte. J Am Chem Soc 2016;138:12258–62.
[147] Luo W, et al. Reducing interfacial resistance between garnet-structured solid-state electrolyte and li-metal anode by a germanium layer. Adv Mater 2017;29:1606042.
[148] Shao Y, et al. Drawing a soft interface: an effective interfacial modification strategy for garnet-type solid-state Li batteries. ACS Energy Lett 2018;3:1212–18.
[149] Han X, et al. Negating interfacial impedance in garnet-based solid-state Li metal batteries. Nat Mat 2017;16:572–9.
[150] Tsai CL, Roddatis V, Chandran CV, Ma Q, Uhlenbruck S, Bram M, Heitjans P, Guillon O. $Li_7La_3Zr_2O_{12}$ interface modification for Li dendrite prevention. ACS Appl Mater Interfaces 2016;8:10617–26.
[151] Taylor NJ, Stangeland-Molo S, Haslam CG, Sharafi A, Thompson T, Wang M, Garcia-Mendez R, Sakamoto J. Demonstration of high current densities and extended cycling in the garnet $Li_7La_3Zr_2O_{12}$ solid electrolyte. J Power Sources 2018;396:314–18.
[152] Cheng L, Park JS, Hou H, Zorba V, Chen G, Richardson T, Cabana J, Russo R, Doeff M. Effect of microstructure and surface impurity segregation on the electrical and electrochemical properties of dense al-substituted $Li_7La_3Zr_2O_{12}$. J Mater Chem A 2014;2:172–81.
[153] Cheng L, et al. The Origin of high electrolyte–electrode interfacial resistances in lithium cells containing garnet type solid electrolytes. Phys Chem Chem Phys 2014;16:18294–300.
[154] Cheng L, Chen W, Kunz M, Persson K, Tamura N, Chen G, Doeff M. Effect of surface microstructure on electrochemical performance of garnet solid Electrolytes. ACS Appl Mater Interfaces 2015;7:2073–81.
[155] Cheng L, et al. Interrelationships among grain size, surface composition, air stability, and interfacial resistance of Al-substituted $Li_7La_3Zr_2O_{12}$ solid electrolytes. ACS Appl Mater Interfaces 2015;7:17649–55.
[156] Han F, Yue J, Chen C, Zhao N, Fan X, Ma Z, Gao T, Wang F, Guo X, Wang C. Interphase engineering enabled all-ceramic lithium battery. Joule 2018;2:497–508.
[157] Wang R, et al. High-temperature ultrafast sintering: exploiting a new kinetic region to fabricate porous solid-state electrolyte scaffolds. Adv Mater 2021:2100726 n/a.
[158] Kamaya N, et al. A lithium superionic conductor. Nat Mater 2011;10:682–6.
[159] Kato Y, Hori S, Saito T, Suzuki K, Hirayama M, Mitsui A, Yonemura M, Iba H, Kanno R. High-power all-solid-state batteries using sulfide superionic conductors. Nat Energy 2016;1:16030.
[160] Sakuda A, Hayashi A, Ohtomo T, Hama S, Tatsumisago M. All-solid-state lithium secondary batteries using licoo2 particles with pulsed laser deposition coatings of Li_2S–P_2S_5 solid electrolytes. J Power Sources 2011;196:6735–41.
[161] Kim DH, Oh DY, Park KH, Choi YE, Nam YJ, Lee HA, Lee SM, Jung YS. Infiltration of solution-processable solid electrolytes into conventional Li-ion-battery electrodes for all-solid-state Li-ion batteries. Nano Lett 2017;17:3013–20.
[162] Kerman K, Luntz A, Viswanathan V, Chiang YM, Chen Z. Review-practical challenges hindering the development of solid state Li ion batteries. J Electrochem Soc 2017;164:A1731–44.
[163] Fu J. Fast Li+ ion conducting glass-ceramics in the system Li_2O–Al_2O_3–GeO_2–P_2O_5. Solid State Ionics 1997;104:191–4.
[164] Lithium-ion conducting glass-ceramics (LiCGC™), Https://www.Oharacorp.Com/LiCGC.Html.
[165] Gellert M, Gries KI, Yada C, Rosciano F, Volz K, Roling B. Grain boundaries in a lithium aluminum titanium phosphate-type fast lithium ion conducting Glass ceramic: microstructure and nonlinear ion transport properties. J Phys Chem C 2012;116:22675–8.
[166] Paolella A, et al. Enabling high-performance nasicon-based solid-state lithium metal batteries towards practical conditions. Adv Funct Mater 2021;31:2102765.
[167] Wu J, Chen L, Song T, Zou Z, Gao J, Zhang W, Shi S. A review on structural characteristics, lithium ion diffusion behavior and temperature dependence of conductivity in perovskite-type solid electrolyte $Li_{3x}La_{2/3-X}TiO_3$. Funct Mater Lett 2017;10:1730002.
[168] Fujiwara Y, Taishi T, Hoshikawa K, Kohama K, Iba H. Anisotropy of ionic conduction in single-crystal Lixla(1−X)/3nbo3solid electrolyte grown by directional solidification. Jpn J Appl Phys 2016;55:090306.
[169] Gao X, Fisher CAJ, Kimura T, Ikuhara YH, Kuwabara A, Moriwake H, Oki H, Tojigamori T, Kohama K, Ikuhara Y. Domain boundary structures in lanthanum lithium titanates. J Mater Chem A 2014;2:843–52.
[170] Lee JZ, Wang Z, Xin HL, Wynn TA, Meng YS. Amorphous lithium lanthanum titanate for solid-state microbatteries. J Electrochem Soc 2016;164:A6268–73.
[171] Jiang Z, Wang S, Chen X, Yang W, Yao X, Hu X, Han Q, Wang H. Tape-casting $Li_{0.34}La_{0.56}TiO_3$ ceramic electrolyte films permit high energy density of lithium-metal batteries. Adv Mater 2020;32:1906221.
[172] Kaboli S, Demers H, Paolella A, Darwiche A, Dontigny M, Clément D, Guerfi A, Trudeau ML, Goodenough JB, Zaghib K. Behavior of solid electrolyte in Li-polymer battery with nmc cathode via *in-situ* scanning electron microscopy. Nano Lett 2020;20:1607–13.
[173] Wang C, Wang T, Wang L, Hu Z, Cui Z, Li J, Dong S, Zhou X, Cui G. Differentiated lithium salt design for multilayered peo electrolyte enables a high-voltage solid-state lithium metal battery. Adv Sci 2019;6:1901036.
[174] Lu J, et al. 4.2 V poly(ethylene oxide)-based all-solid-state lithium batteries with superior cycle and safety performance. Energy Storage Mater 2020;32:191–8.
[175] Qiu J, et al. Enabling stable cycling of 4.2 V high-voltage all-solid-state batteries with peo-based solid electrolyte. Adv Funct Mater 2020;30:1909392.
[176] Liang J, et al. Insight into prolonged cycling life of 4 V all-solid-state polymer batteries by a high-voltage stable binder. Adv Energy Mater 2021;11:2002455 2002455.
[177] Mauger A, Julien CM. Review of 5-V electrodes for Li-ion batteries: status and trends. Ionics 2013;19:951–88.
[178] Ponnuchamy, V. Towards a better understanding of lithium ion local environment in pure, binary and ternary mixtures of carbonate solvents: a numerical approach
[179] Etude Théorique Et Numérique De L'interaction Des Ions Lithium Dans Les Solvants Carbonates Et Leurs Mélanges. Université Grenoble Alpes; 2015.
[180] Logan ER, Tonita EM, Gering KL, Ma L, Bauer MKG, Li J, et al. A study of the transport properties of ethylene carbonate-free Li electrolytes. J Electrochem Soc 2018;165(3):A705–16.
[181] Xu K. Electrolytes and Interphases in Li-ion batteries and beyond. Chem Rev 2014;114:11503–618.
[182] Zhang W, Xia H, Zhu Z, Lv Z, Cao S, Wei J, Luo Y, Xiao Y, Liu L, Chen X. Decimal solvent-based high-entropy electrolyte enabling the extended Survival temperature of lithium-ion batteries to −130 °C. CCS Chem 2021;3:1245–55.
[183] Chiba K, Ueda T, Yamaguchi Y, Oki Y, Saiki F, Naoi K. Electrolyte systems for high withstand voltage and durability ii. alkylated cyclic carbonates for electric double-layer capacitors. J Electrochem Soc 2011;158:A1320.
[184] Awwad AM, Al-Dujaili AH, Salman HE. Relative permittivities, densities, and refractive indices of the binary mixtures of sulfolane with ethylene glycol, diethylene glycol, and poly(ethylene glycol) at 303.15 K. J Chem Eng Data 2002;47:421–4.
[185] Hilbig P, Ibing L, Wagner R, Winter M, Cekic-Laskovic I. Ethyl methyl sulfone-based electrolytes for lithium ion battery applications. Energies 2017;10:1312.
[186] Kumar N, Siegel DJ. Interface-induced renormalization of electrolyte energy levels in magnesium batteries. J Phys Chem Lett 2016;7:874–81.
[187] Xu K. Nonaqueous liquid electrolytes for lithium-based rechargeable batteries. Chem Rev 2004;104:4303–418.
[188] Xu K, Zhang S, Jow TR, Xu W, Angell CA. Libob as salt for lithium-ion batteries: a possible solution for high temperature operation. Electrochem Solid State Lett 2002;5:A26.
[189] Zhou ZB, Takeda M, Fujii T, Ue M. Li[C[Sub 2]F[Sub 5]Bf[Sub 3]] as an electrolyte salt for 4 V class lithium-ion cells. J Electrochem Soc 2005;152:A351.